Dynamics of chlorophyll *b* in the photosystems of *Arabidopsis thaliana*

（シロイヌナズナにおけるクロロフィル *b* の動態）

by

Ting JIA

A Dissertation Submitted to the Graduate School of Life Science, Hokkaido University in partial fulfillment of the Requirements for the Degree of Doctor of Philosophy in Life Science

Laboratory of Plant Adaptation Biology

Graduate Course of Biosystem Science

Graduate School of Life Science

Hokkaido University

March, 2016

Contents

General Abstract

In the chlorophyll cycle, chlorophyll *b* is synthesized from chlorophyll *a* (forward reaction) by chlorophyllide *a* oxygenase (CAO) and chlorophyll *b* is reconverted to chlorophyll *a* (backward reaction) by chlorophyll *b* reductase (NOL, NYC1) and 7-hydroxyl chlorophyll *a* reductase (HCAR). Activity of the forward and backward reactions alters the levels of chlorophyll *a* and chlorophyll *b* which is associated with the changes of chlorophyll *a*/*b* ratio. The level of light harvesting complexes, which forms the antenna of photosystem II (PSII), is primarily regulated by the chlorophyll cycle. Stabilization of light harvesting chlorophyll *a*/*b* binding protein complexes (LHCII) is corelated with accumulation of chlorophyll *b* indicating that LHCII formation is regulated by chlorophyll *b* synthesis. In contrast, degradation of chlorophyll *b* is the initial step of LHCII degradation during senescence, indicating that chlorophyll *b* degradation regulates the degradation of LHCII. This study aimed to clarify the regulation mechanisms of the formation and degradation of LHCs by the chlorophyll cycle. In the first part, I examined detail of LHCII formation and its effect on the structure and stoichiometry of both photosystems when chlorophyll *b* synthesis was triggered by the expression of the full length CAO in the *Arabidopsis* chlorophyll *b* less mutant *ch1-1*. Out results show that accompanied with biosynthesis of chlorophyll *b*, LHCs apoproteins were accumulated. Formation of LHCII trimer was associated to the core antenna of PSII to form PSII-LHCII supercomplexes. Peripheral antenna of photosystem I (PSI) and II increased after chlorophyll *b* synthesis. I also found that PSI/PSII ratio was altered accompanied by the synthesis of chlorophyll *b*. In the second part, I examined the effect of chlorophyll *b* on the accumulation NYC1 which is responsible for the degradation of LHCII during leaf senescence. In this study, I introduced BC domain of CAO fused with GFP into *Arabidopsis* mutant *ch1-1*,

which was named BCG plant, in which chlorophyll *b* was over-produced. Analysis of my results show that NYC1 was over-accumulated in BCG plant, but not in *ch1-1* after dark incubation; however, the mRNA level increased in both BCG and *ch1-1* after dark incubation. Interestingly, LHCII protein level did not corelate with NYC1 protein level; chlorophyll fluorescence of dark adapted plant (Fo) displayed high co-relationship with accumulation of NYC1 suggesting NYC1 level is related to the energetically uncoupled LHC.

General introduction

Chlorophyll serves as critical role in photochemistry by absorbing solar irradiance and transferring light energy or electron to other molecules. There are several remarkable variations of chlorophyll species both in terrestrial and aquatic environment. Land plants, green algae and a few groups of cyanobacteria have two types of chlorophyll, chlorophyll *a* and chlorophyll *b* (Figure 1). Chlorophyll *a* has a methyl group in side chain at C7 position, whereas, the methyl group is replaced by formyl group in chlorophyll *b*.

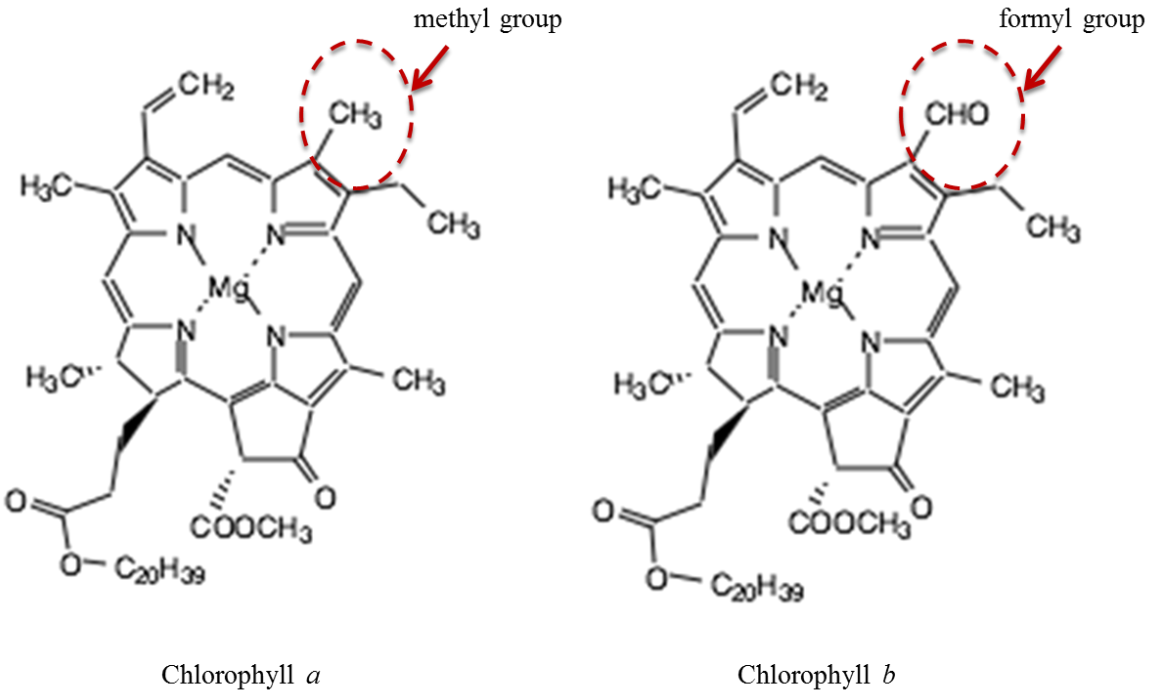

Chlorophyll *a* Chlorophyll *b*

Figure 1. Molecular structure of chlorophyll *a* and chlorophyll *b*

It has been well known in chlorophyll biosynthesis, which begins with the reduction of glutamyl-tRNA into glutamate-1-semialdehyde and follows by subsequent enzymatic reactions to synthesize chlorophyll *a* (1). Then a portion of chlorophyll *a* in chlorophyll *a* pool is converted to chlorophyll *b* by two reaction steps via 7-hydroxymethyl chlorophyll *a* (HMChl) catalyzed by a Rieske-type monooxygenase that was named chlorophyllide *a* oxygenase (CAO) (2). Chlorophyll *a* to chlorophyll *b* is interconversion in oxygenic photosynthetic organisms and vice visa. Chlorophyll *b* is converted to chlorophyll *a* by chlorophyll *b* reductase (NOL, NYC1) (3) and 7-hydroxyl chlorophyll *a* reductase (HCAR) (4) (Figure 2) which is necessary for chlorophyll *b* degradation. .

Formation and degradation process of chlorophyll *b* form integral chlorophyll cycle. Chlorophyll *b*, of which role as a regulator in photosynthetic antenna, keeps fluctuation demonstrating the change in chlorophyll *a*/*b* ratio to increase or

decrease photosynthetic antenna size to capture enough light supplying energy for plants metabolism in environmental irradiance. Theoretically, change of chlorophyll *a*/*b* ratio can be determined by the activity both in forward and backward reactions in chlorophyll cycle (5). Over-expressing catalytic domain of CAO fused with GFP (BCG plant) results drastically in the decrease of chlorophyll *a*/*b* ratio from approximately 3.0 to about 1.0 (6). And in *Arabidopsis* mutant *nyc1*, chlorophyll *a*/*b* ratio was around 1.0 by contrast with wide type after dark incubation (7). Both in BCG and *nyc1*, LHCII are stabilized. These data indicate that chlorophyll *b* is closely corelated with LHCII stabilization. In this thesis, I further analyzed the relationship between chlorophyll metabolism and LHCII through the forward and backward activity in chlorophyll cycle respectively using different transgenic plants, in which chlorophyll *b* can accumulate.

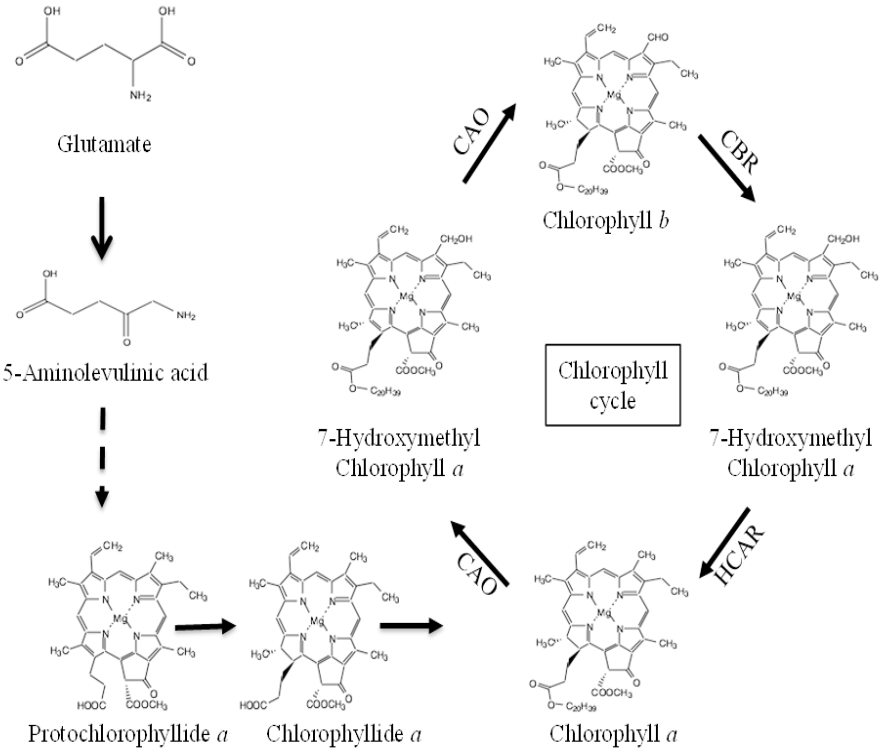

Figure 2. Chlorophyll biosynthesis pathway

Chapter 1 Role of chlorophyll *b* in photosynthetic acclimation in *Arabidopsis thaliana*

Abstract

Photosynthetic efficiency dependents on coordination of photosystem II (PSII) and photosystem I (PSI) by changing the composition, structure and function of their apparatus in response to various environmental irradiances. These changes require both long time scale and short time scale responses. It has been suggested that both long time and short time response are involved in signaling from redox plastoquinone pool (PQ). In this study, I found a novel characteristic of chlorophyll *b* in environmental adaption by inducing CAO in *Arabidopsis* mutant *ch1-1*.The results showed that synthesis of chlorophyll *b* in *Arabidopsis* mutant *ch1-1*, which is CAO deficient mutant and lacks of chlorophyll *b*, by transiently over-expressing CAO induced increase of newly synthesized light-harvesting chlorophyll *a*/*b* binding-protein complexes I (LHCI) and II (LHCII), and LHCI, LHCII respectively associated with PSI and PSII as a functional peripheral antenna. Lhcb1 and Lhcb2 were phosphorylated and non-photochemical quenching (NPQ) which can dissipate excess energy increased during synthesis of chlorophyll *b*. I also found the increase of CP1 (main component of PSI) and slight decrease of CP43 (one of components for core antenna in PSII) indicating the changes in the amount of PSI and PSII reaction centers induced by energy distribution imbanlance between two photosystems. These results clearly show that synthesis of chlorophyll *b* enhanced the NPQ and state transition, changed the stoichiometry of two photosystems indicating that chlorophyll *b* plays a critical role during photosynthetic acclimation.

1.1 Introduction

Survival of plants on earth relies on solar energy, and photosynthesis is the only biological process able to harvest this energy. However, plants cannot escape from various environmental changes which directly affect photosynthetic reactions. To protect against environmental stress and to maintain optimal photosynthetic efficiency, plants have developed the adaptation mechanisms, one of which is related to balance photo-excitation between two photosystems by modulating the photosynthetic apparatus. As photosynthetic apparatus, LHCI and LHCII associating PSI and PSII respectively harvest light energy, while PSI and PSII work in serial to transform light energy to chemical energy (8). The apparatus act either as energy dissipaters to dissipate exceeded energy or as energy collectors to absorb more light (9). Regulation of photosynthetic apparatus is dependent on two acclimation time-scale, one is called short term response, which rearrange structure of two photosystems to modulate light absorption (10), another is long term response, which re-adjust photosynthetic stoichiometry in favor structural components of photosystems (11). Short term response occurs in seconds or minutes so that there is no time to synthesis new chlorophyll-protein or electron transport proteins while longer term response occurs in hours or days that require synthesis and assemble of new membrane components and degradation of other components (12). Plants has complicated network to mediate these time-scale responses to adapt inhabits.

The best documented evidence for short term response is studies dealing with reversible phosphorylation (12). A mobile pool of LHCII existing in plants serves as switch to modulate the light-harvesting antenna size in order to balance excitation energy between PSI and II, this switch terms as state transition involving in movement portion of phosphorylated/de-phosphorylated LHCII (13). When reduced plastoquinone (PQ) pool transfers electron from PSII to cytochrome b_6f

(cyt b_6f) complex, a redox sensitivity kinase (STN7) is activated to phosphorylate the mobile LHCII (14, 15), this results in the LHCII is detached from PSII and attached to PSI. when PQ pool is oxidized, another redox sensitive phosphatase (PPH1/TAP38) are activated to de-phosphorylate the LHCII inducing re-association of the LHCII to PSII (16, 17). Signal from redox state PQ pool triggers the state transition to mediate decrease or increase of antenna size of two photosystems in order to re-balance the excitation energy between two photosystems.

Non-photochemical quenching (NPQ) is another important short-term acclimation (18) process being able to increase in plant tolerance. Function of NPQ is to prevent plants from photo damage by dissipating excess solar energy to heat via light-harvesting antenna in higher plants and green algae (19, 20). Site of NPQ is located in LHCII (21) and down-regulation of NPQ was observed in the *Arabidopsis* mutant *ch1-1*, which retains only minor light-harvesting complex component Lhcb5 among ten light-harvesting complexes of plants (22). It has proved that NPQ occurs coupled with state transition via STN7 kinase in the control of chloroplast redox balance upon fluctuating light (23).

By contrast with movement of LHCII from mobile pool during state transitions in short term response, adjustment of photosystem stoichiometry start with the perception of imbalances in excitation energy by changing the relative amounts of the two photosystems via reduction／oxidation (redox) signals from the photosynthetic electron transport chain, and this process requires hours and days (24–26). However, photosystem stoichiometry change is highly conserved in nature, because the mechanism of this phenomenon is well known to involve in oxygen evolution organisms in land plants (27) and accumulation of chlorophyll *a* and chlorophyll *b* (28).

Both state transition and adjustment of photosystem stoichiometry are related to redox signal from PQ pool and work to enhance the electron transport capacity of the rate-limiting photosystem even if these two processes have different time-scale, however, it is still debated for the regulatory mechanism of this coupling processes. Chlorophyll *a*/*b* ratio exhibited characteristic difference in state transition (29), variation of photosystem stoichiometry (30) and change of antenna size (31). As an indispensable pigment existing only in peripheral antenna, I presume chlorophyll *b* is involved in photosynthetic acclimation.

In this report, I transiently induced *CAO* in *Arabidopsis* chlorophyll *b* less mutant *ch1-1*, in which *CAO* was deleted and accumulation of peripheral antenna were low level by contrast with *Arabidopsis* WT, and measured the change of antenna size. My results showed that peripheral antenna size both in PSI and PSII increased, and simultaneously number of reaction center in two photosystems changed indicating that synthesis of chlorophyll *b* is involved in adjusting peripheral antenna size and reaction center number of two photosystems.

1.2 Results and Discussion

1.2.1 Both pre-existing chlorophyll *a* and newly synthesized chlorophyll *a* are substrate of CAO

Arabidopsis CAO contains three domains: the “A” domain stabilizes synthesized CAO protein; the “B” domain links “A” and “C” domain; “C” domain catalyzes the conversion of chlorophyll *a* to chlorophyll *b* (32). When “B” and “C” domain were fused with GFP and expressed in *ch1-1*, chlorophyll *b* was excessively produced and chlorophyll *a*/*b* ratio decreased to about 1.5 (6). It was also reported that when *Prochlorothrix hollandica* CAO, a prokaryotic chlorophyll *b* synthesis

gene, was induced in *ch1-1* under low light condition, chlorophyll *a*/*b* ratio was around 1.1 by contrast with WT, in which the chlorophyll *a*/*b* ratio are usually around 3.0, and chlorophyll *b* was accumulated both in peripheral and inner antenna (33). Here, I transiently induced the full length of CAO in 4 week-old *Arabidopsis* mutant *ch1-1* using dexamethasone (Dex).

Theoretically, there are two distinct pools of chlorophyll *a* molecule that could be used for chlorophyll *b* biosynthesis, one is pre-existing chlorophyll *a*, which exists in chlorophyll protein complex, such as CP47 and CP43; another is newly synthesized chlorophyll *a*. First, I examined whether pre-existing chlorophyll *a* can be a substrate for CAO. Plants were grown on MS agar in grow light (16 h light/ 8 h dark) for 20 days, then the plants were transferred to MS agar containing Dex, and immediately put in the dark to inhibit chlorophyll *a* synthesis. The conversion of protochlorophyllide *a* to chlorophyllide *a* is light-dependent step. When plants are incubated in darkness, this step is completely inhibited, thus chlorophyll *a* is not newly synthesized under this condition. After 5 days of dark incubation, chlorophyll content was examined by HPLC. Figure 3 showed that chlorophyll *b* was synthesized in Dex treated line although the level was low, but not in untreated line. The results clearly show that pre-existing chlorophyll *a* can be also converted to chlorophyll *b* by CAO.

Next, we examined the chlorophyll *b* synthesis under light condition where newly synthesized chlorophyll is supplied. Figure 4A shows phenotype of three independent CAO overexpressing homozygotes after Dex treatment. Compared with WT, the leaf color of over-expression lines was pale green before Dex treatment; after 4 days of Dex treatment, leaf color became dark green. Then I measured the chlorophyll *a*/*b* ratio before and after Dex treatment. Chlorophyll *a*/*b*

ratio gradually decreased during Dex treatment (Table 1). Because line 6 had the lowest chlorophyll *a*/*b* ratio, I used line 6 for further experiments.

Chlorophyll *a*/*b* ratio was changed to adjust the antenna size in photosystems under various light intensities in *Arabidopsis* (34). However, our knowledge for the mechanism of controlling chlorophyll *a*/*b* ratio is still limited. When *Arabidopsis* CAO containing B and C domain and fusing with GFP was over-expressed in *ch1-1*, chlorophyll *a*/*b* ratio was around 2.2, which was further lower than in WT; similar when *Prochlorothrix hollandica* CAO was induced in *ch1-1* (6, 35). In my experiment, the chlorophyll *a*/*b* ratio was decreased from 1 to 4 days after Dex treatment, but was still higher than in WT. Possible reason is that it might take a long time to reach similar chlorophyll *a*/*b* ratio with in WT after CAO was transiently induced in *ch1-1*, but we just picked up samples from 1 to 4 days. An interesting phenomenon was also observed that accompanied with chlorophyll *b* accumulation, the amount of chlorophyll *a* also increased. It is probably because plants strictly regulate the chlorophyll *a*/*b* ratio to operate optimal energy transfer and keep a fixed stoichiometry. Regulation of chlorophyll synthesis can be monitored by examining some gene expression which is involved in chlorophyll biosynthesis. Glu-tRNA reductase, which is encoded by *HemeA1* and catalyzes a committed step in chlorophyll biosynthesis pathway, can be used to evaluate the regulation role in chlorophyll biosynthesis pathway. HemeA1gene expression was higher in 2 days than in 1day or 4 days after Dex treatment (Table 2), the result was coincident with the increase in biosynthesis of the content of chlorophyll *a* and *b*.

To further confirm the induction of CAO, I performed RT-PCR to examine expression level of *CAO*. *CAO* expression level was higher after Dex treatment than in WT (Figure 4B). Interestingly, CAO level gradually decreased from 6

hours to 1.5days of Dex treatment, some unknown stress might exist to affect CAO expression during this time course. The level arrived to maximum after 2 days of Dex treatment, and then decreased. This result was corresponding with chlorophyll *b* accumulation (Figure 5). Chlorophyll *b* was detected after 12 hours of Dex treatment and the content gradually increased until 3.5 days of Dex treatment. However, amount of chlorophyll *b* were not significantly different from 2 to 3.5 days of Dex treatment. At 4 days of Dex treatment, accumulation of chlorophyll *b* drastically decreased.

1.2.2 Accumulation of chlorophyll *b* induce accumulation of peripheral antenna apoproteins

It has been proved that constitutively over-expressing CAO in *ch1-1* can enhance accumulation of LHC protein upon light acclimation (36). Here I transiently induced CAO in *ch1-1* and examined the accumulation of photosynthetic apoproteins using immune blotting. The results showed that level of CP43 and D1 proteins were similar among *CAO* over-expressing line treated with or without Dex and WT (Figure 6). All of LHC apoproteins were accumulated after Dex treatment except Lhca2 and Lhcb5 protein, these two proteins exists in *ch1-1*, and the content is almost constant after Dex treatment. CP1 protein reached to maximum level at 4 days of Dex treatment and the level was almost equal with in WT. Result of microarray analysis (Table 2) showed stable expression level of Lhca1-4 and Lhcb1-6 before and after Dex treatment. These results further prove the conclusion in previous report that *CAO* is involved in the regulatory mechanism of LHC accumulation (36).

Barley chlorophyll *b*-less mutant (*chlorina*) lacked the majority of light-harvesting complexes (LHC) (37) and turnover rate of several LHC proteins increased (38),

more specifically, accumulation of LHC apoproteins (Lhcb1-Lhcb6 and Lhca1-Lhca4) were significantly reduced in this mutant (39). Bossman et al reported that chlorophyll *b* levels correlated with LHC protein levels after examined ten different alleles of *chlorine* (40), similar result was obtained in *Arabidopsis* (41, 42). In my results, LHCs proteins accumulated concomitant with chlorophyll *b* accumulation, but LHCs genes expression were constant irrespective of Dex treatment. These data are consistent with previous finding that chlorophyll *b* must be embedded in LHCs apoproteins to stabilize LHCs proteins. it was reported that there are 6 Lhcb (Lhcb1-Lhcb6) and four Lhca (Lhca1-Lhca4) proteins consisting in peripheral antenna of PSII and I respectively in *Arabidopsis* (43).

1.2.3 Accumulated LHC protein assemble to core antenna to form integrated photosystems

In the next step of my study, I investigated whether the accumulated LHCs protein attached to core antenna or not. Firstly, I performed blue native PAGE to detect PSII-LHCII supercomplexes. Figure 7 displayed that LHCII trimer was detected after 1 day of Dex treatment and PSII-LHCII supercomplex was formed at 1.5 days after Dex treatment. It means newly synthesize LHCII trimer was successfully associated to PSII accompanied with accumulation of chlorophyll *b*. LHCII trimer decreased from 1.5 to 2 days and PSII-LHCII supercomplexes were almost constant. As a major LHCII protein, Lhcb1-Lhcb3 are present as heterotrimeric form whereas minor LHCII (Lhcb4-Lhcb6) exist in monomeric form (44). Moreover, the heterotrimeric LHCII can associate with dimeric PSII core complexes via minor LHCII which function as a linker (45). All of the LHCII apoproteins were accumulated after Dex treatment, and clearly LHCII trimer was found after 1 day of Dex treatment and PSII-LHCII supercomplexes was detected at 1.5 days of Dex treatment. It is reasonable that firstly chlorophyll *b* is

synthesized and chlorophyll-protein complexes are formed, then the major complexes aggregated to heterotrimeric form and assembled to dimeric PSII core complexes via minor complexes. Same process occurred in LHCI.

Then I measured fluorescence emission spectra of PSII and PSI at liquid nitrogen temperatures. The wavelength of the peak of fluorescence spectra of PSI was red-shifted from 725nm to around 735 nm after Dex treatment, simultaneously fluorescence intensity was increased but still lower than WT (Figure 8). Lhca1/4 and Lhca2/3 form red-emitting heterodimers respectively (46), which is consistent with the immune blotting results that Lhca2 and Lhca3 retained but Lhca1 and Lhca4 were deficient in *ch1-1*. In Lhca4 mutant, Lhca4 and Lhca1 were completely absent and less than 0.1% of Lhca2 and Lhca3 were detected, and the mutant exhibited red emission at around 720nm. In Lhca1 mutant, the amount of Lhca2 and Lhca3 were constant with WT but, content of Lhca1 and Lhca4 were less than 0.1% and the mutant exhibited red emission at around 732nm (47), in my experiment, the red emission was around at 725nm, which is reasonable because the levels of Lhca2 and Lhca3 in *ch1-1*were lower than in WT. The emission fluorescence might be partly derived from P700 and existing Lhca2 and Lhca3. The red chlorophyll a603-a609 dimers existing in each Lhca subunit (48) contribute low temperature fluorescence. After Dex treatment, the fluorescence intensity also increased, so I speculate that the site for red chlorophyll a603/a609 was reoccupied by newly synthesized chlorophyll accompanied with accumulation LHCI. These results together clearly indicate that newly synthesized LHCs by Dex treatment were successfully associated to PSI and PSII core complexes respectively to form integrated photosystems.

1.2.4 Newly synthesized peripheral antennas are functional and the size increase

To confirm whether the newly synthesized peripheral antennas in PSI and PSII can harvest light or not, I also measured the functional antenna size of PSI and PSII using dual PAM system. The rate coefficient of P700 photooxidation by steady far-red light when electron simultaneously transferred from PSII to $P700^+$ after a flash can be used to evaluate relative antenna size of PSI. Figure 9A showed time course of $[P700^+]$ induction according the equation: $[P700^+] = \exp(-K_{red}*t)+y_{ss*}[1-\exp(-K_{ox}*t)]$. By this equation, I got the rate coefficient Kox, which was constant in steady far-red light, implied the relative antenna size of PSI. After Dex treatment, Kox gradually increased and reached to the value similar with WT at 2 days of Dex treatment, Kox from 3 days of Dex treatment was almost similar with WT (Figure 9B).

To measure PSII relative antenna size, I used DCMU-poisoned leaf to assume to be proportional the quanta number which is utilized in photochemical work by PSII reaction center. In previous report, a fast exponential α-component and a slower exponential β-component were used to describe the primary photochemistry of two types of PSII reaction center, but the β-component displayed an inefficient coupling to light-harvesting pigment, either a small absorption of cross section (49). Thus, in this experiment, I only used α-component to indicate relative antenna size of PSII. In Figure 10, A and B showed kinetics analysis of normalization curve and α-, β-component curve from WT and *ch1-1*. K_α and K_β can be obtained by fitting the fluorescence curve, which was calculated from following formula: $A(t) = \alpha_{Max*}(1-\exp(-K_\alpha*t)) + \beta_{Max}*(1-\exp(-K_\beta*t))$, to normalize fluorescence curve. K_α was increased after Dex treatment, the Kα was maximum level at 2 days of Dex treatment and it was not significantly different from 2 to 4 days of Dex treatment, but Kα was still lower than that in WT (Figure 10C). After Dex treatment, relative antenna size of PSI reached to the same level of WT while relative antenna size of

PSII was still smaller than that of WT. In my view, one reason for imbalance of the increase in antenna size between the two photosystems is that synthesized chlorophyll *b* is not sufficient to from LHCII as in WT resulting in the smaller PSII antenna but PSI antenna requires smaller chlorophyll *b* which enable complete antenna with a small amount of chlorophyll *b*. However, these responses will produce imbalance of excitation status of the two photosystems. Then a question arises as to how the plant coops with these unbalance. In order to answer this question, we measured the numbers of photosystems.

1.2.5 Accumulation of chlorophyll *b* induce change of photosynthetic stoichiometry

Figure 6 showed change of CP1 and CP43 protein level during Dex treatment. So I used a serial dilution (12.5, 25, 50, 100%) to quantify the relative content of CP1 and CP43 (Figure 11A). The results showed that CP1 protein increased but CP43 protein decreased when chlorophyll *b* was synthesized. The ratio of CP1/CP43 was used to evaluate change of stoichiometry in two photosystems. CP1/CP43 ratio was lower in *ch1-1* than in WT (Figure 11B). The ratio was increased from 1 day to 4 day after Dex treatment, but was still lower than in WT because CP1 protein level in one experiment at 4 days was still less than in WT. This data indicates that change of PSII core antenna size and PSI core were not because stoichiometry change between PSI and PSII. Thus, I think that the amount of reaction centre of PSI and PSII were changed when chlorophyll *b* was synthesized.

To analyze the content of PSI, the amount of P700 was determined in solubilized thylakoids using spectrophotometer to measure absorption changes at 700 nm. The number of chlorophyll/P700 reaction centre was estimated to be around 250 in WT and 375 in the *ch1-1* (Figure 12). This result is different with reported result, in

which in chlorophyll/P700 was around 600, so I was trying to improve the experimental method in order to get reliable result. Chlorophyll/P700 reaction centre was increased after Dex treatment. Loss of LHCII is partly counter-balanced by a decrease in the number of PSI complexes in rice *chlorina* mutant (50). In *Arabidopsis ch1-1*, chlorophyll/P700 was higher than in WT. Increased amount of LHCII timer causes decrease of PSI reaction center per chlorophyll resulting in the increase in chlorophyll/P700. Same samples were used to measure chlorophyll/cytochrome b559 which indicates amount of PSII reaction center by measuring absorption at 559nm. Number of chlorophyll /cytochrome b559 in WT was about 2 times higher than in *ch1-1*. After 1 day of Dex treatment, the number were almost similar with WT, then drastically decreased and keep constant with in *ch1-1* from 2 days to 4 days after Dex treatment. P700/b559 ratio slightly increased from before Dex treatment to after Dex treatment (Figure 12). Together, these data indicate that increase of number of PSI reaction center induced the increase of PSI core. The reason for minor decrease of PSII reaction center might be increase of formation of peripheral antenna size.

1.2.6 Accumulation of chlorophyll *b* triggers state transition

State transition is driven by phosphorylated partial of LHCII in a mobile pool of LHCII (51), recently, it was suggested that LHCII is phosphorylated in long term acclimation response and functional associated to PSI (8). Change of photosynthetic stoichiometry has been evaluated by the protein levels during chlorophyll *b* synthesis (Figure 11), so I supposed that the state transition also occur in this process. As major component of LHCII, Lhcb1 and Lhcb2, can be phosphorylated at a Thr residue which is close to the N terminus by STN7 (15). Thus, I measured the phosphorylated Lhcb1 and Lhcb2 using immunoblotting analysis. Figure 13A shows that phosphorylated Lhcb1 was detected after 1 day of

Dex treatment, little amount of phosphorylated Lhcb2 were detected after 0.5 day of Dex treatment. Level of phosphorylated Lhcb1 and Lhcb2 both increased after Dex treatment but were always lower than accumulation of Lhcb1 and Lhcb2 in Figure 6, which result was consistent with previous report that only part LHCII was phosphorylated.

1.2.7 Biosynthesis of chlorophyll *b* enhances NPQ

NPQ is effective short-term regulatory photo-protection process that can feed-back control of excess light energy in PSII (52). NPQ is constituted with three component, qI, qT and qE. qE, which is the major part of NPQ, develops and relaxes within seconds and/or minutes in high light condition (53, 54). It has been widely accepted that qE quenching is located in LHCII antenna. *ch1-1* displayed a low level of qE quenching before Dex treatment (Figure 13B). The level of qE increased after Dex treatment but was the level was still lower than in WT which might be related to amount of chlorophyll *b*.

1.3 Conclusion

In this study, we found the accumulation of LHCII and LHCI when chlorophyll *b* synthesis was induced by Dex systems. Synthesized LHCs assembled with photosystems to form super complexes of both photosystems. Antenna size of PSI became the same level of WT but that of PSII of Dex treated plants was smaller than that of WT. But the ratio of PSI/PSII particles increased which might balance the excitation status of both photosystems. This suggests that both antenna size and photosystem stoichiometry are simultaneously changed during acclimation, a working model is established in Figure 14.

1.4 Experimental Procedures

1.4.1 Plasmid construction and transformation plants

For the transformation of *Arabidopsis*, a full-length coding sequence of the *Arabidopsis* CAO gene was introduced into the Gateway entry vector pENTR4 Dual and then introduced into the Gateway-compatible inducible vector pOpOn6. Primer set is listed in Table 4. Transgene expression was driven by pOp6 promoter. The construct was introduced into Agrobacterium tumefaciens (strain GV3101) and transformed into *Arabidopsis* mutant *ch1-1*(CAO deficient mutant) using a floral dip method (55). Homozygous of over-expressing transformants were screened by kanamycin resistance.

1.4.2 Plant materials and growth conditions

Arabidopsis thaliana WT (*Columbia*) and transformants plants were grown at 25 ℃ under continues light conditions (24-h light) in chambers equipped with white fluorescent lamps at a light intensity of 80 μmol m^{-2} sec^{-1}. Four to five weeks old transformants were sprayed by 20 μM Dex to transiently induce CAO expression. Fully expanded rosette leaves from 4-week old WT and from 5-week old transformants with and without Dex treated were harvested for experiments. Because *ch1-1*grows slowly than WT.

1.4.3 Pigment analysis

Leaves were weighted and ground in pure acetone which were stored at -20℃using a Shaker Master (biochemical Science)(56). The boxes that used for Shaker master was also pre-cooled in liquid nitrogen. The extracts were centrifuged at 20 000 *g* for 10 min at 4 ℃. Pigment were analyzed using HPLC with a Symmetry C8 column (150 mm in length, 4.6 mm in inner diameter) (Waters) according to previous report (57).

1.4.4 SDS-PAGE and immunoblot analysis

For total protein extraction, the leaf tissues were weighted and ground in liquid nitrogen, then homogenized with protein extraction buffer, which contain 125 mM Tris-HCl (pH 6.8), 4% (w/v) SDS, 10% (w/v) sucrose, and 10% (v/v) 2-mercaptoethanol. One milligram leaf tissues were homogenized with 10 µl extraction buffer. Equal volume of sample buffer, which contain 50 mM Tris-HCl (pH 6.8), 2 mM EDTA, 10% (w/v) glycerol, 2% SDS and 6% 2-mercaptoethanol, was added to the mixture. One point five microliters (for CP1, D1, CP43, CP47) and 2.5 µl (for Lhcb1-6, Lhca1-4) of supernatant were subjected into SDS-PAGE gel, then transferred onto a polyvinylidene difluoride membrane. Anti-rabbit primary antibody against CP1, D1, D2, CP43, CP47, Lhcb1-6, Lhca1-4 were used for immunoblotting analysis. CP1 and CP43 were quantified using IMAGE J software. A serial dilution of an extract from WT was applied on every blotting analysis.

1.4.5 Blue-native PAGE analysis

Blue-native PAGE was performed according to previous report(42, 58). The purified thylakoid membranes (which contain 5 µg of chlorophyll) was isolated from leaf tissues. Leaves tissues were homogenized by ice cooled glass homogenizer in grinding buffer containing 0.45 M sorbitol, 20 mM Tris/KOH pH8.4, 10 mM EDTA, 10 mM $NaHCO_3$ and 0.1% (w/v) BSA . Homogenate was filtered by 4 layer pore mesh filter, then was centrifuged at 4000 *g* at 4℃ for 4 min. The supernatant was discarded and pallet was washed twice with washing buffer containing 0.3 M sorbitol, 20 mM Tricine/KOH pH7.6, 5 mM $MgCl_2$ and 2.5 mM EDTA. The pallet was re-suspended with solubilization buffer containing 50 mM imidazole-HCl (pH 7.0), 20% glycerol, 5 mM 6-aminocaproic acid and 1 mM

EDTA, then was mixed with 2% (w/v) α-DM. After centrifugation at 20000 *g* at 4℃ for 5 min, supernatants were supplemented with 5% (w/v) CBB Serva Blue G, 500 mM 6-aminocaproic acid and 50 mM imidazole-HCl (pH 7.0). Solubilized membrane proteins were separated by 4- 14% acrylamide gradient gels.

1.4.6 Low Temperature fluorescence measurement

Leaves were cut and immediately put into glass tube and then into liquid nitrogen. Fluorescence emission spectra were obtained at 77 K by using fluorescence spectrophotometer (F-2500, Hitachi). The wavelength of blue excitation light was 465 nm with slit width of 2.5 nm and emission was obtained through slit width 2.5 nm with speed of 300 nm s^{-1}. Excitation spectrum was measured by monitoring at the 690 nm and 730 nm fluorescence peak of PSII and PSI, respectively.

1.4.7 PSI and PSII antenna size measurement

Photo-oxidation and re-reduction of P700 in leaf tissues were examined using pulse amplitude modification PAM system (Dual-PAM-100, Walz), which with a dual wavelength (830/870 nm) unit or a single wavelength (730 nm) and attached to a pulse amplitude modulation fluorometer. A leaf that cut from plants was immediately illuminated in far-red light until P700 was steadily oxidized to $P700^+$, then the observed maximum signal was used as a total amount of $P700^+$, and normalized to give the oxidation of P700 fraction at any instant. According to previous report (59), by fitting the time course of $P700^+$ following equation below: $[P700^+]=\exp(-K_{red}t)+yss[1-\exp(-K_{OX}t)]$ coefficient rate K_{OX} at constant far-red light indicates the relative antenna size of PSI.

Leaves were cut from plants and treated by 160 μM DCMU with 0.1% (w/v) Tween 20. Fluorescence was measured by dual PAM system at actinic light

intensity 5 to assure maximal fluorescence yield. The fluorescence trace was normalized using following equation: $Fv(t) = K_{\alpha}*Amax*(1 - e^{-K\alpha*t})+ K_{\beta}*Bmax*(1 - e^{-K\beta*t})$in Melis and Homann's report (49). Fluorescence curve of PSII consistent with two time course of relative logarithmic area: first linear phase and second linear phase. Because *ch1-1* only has the first linear phase, so I used the respective slope of first phase Kα in logarithmic plot to indicate the relative antenna size of PSII.

1.4.8 Chlorophyll/P700 and chlorophyll/cytochrome b559 measurement

Thylakoid member were isolated from leaf tissues which were homogenized in isolation buffer containing 10 mM Tris-HCl PH7.5, 10 mM NaCl and 30 mM sucrose using pre-cooled glass homogenizer. The extract were filtrated by pore mesh filter, then centrifuged at 20000 *g* at 4℃ for 15 min. The pallet were re-suspended by 0.2% TrionX-100, and centrifuged at 20000 *g* at 4℃ for 10 min.

P700 concentration was examined from the different absorption spectra between 0.3 mM ferricynide supernatant and 5 mM ascorbate supernatant by spectrophotometer (U3010, Hitachi) using extinction coefficient 64 mM^{-1} (60). Cytochrome b559 concentration was measured from the different spectra between 8 mM hydroquinone supernatant and 5 mM ascorbate supernatant by spectrophotometer. The same solution was used to measure P700, cytochrome b559 and the chlorophyll concentration by Zapata's report (57).

1.5 Tables, figures and legend

Table 1. Chlorophyll content and chlorophyll *a*/*b* ratio

in WT and different transformants

	line	Chl *a* (nmol/g)	Chl *b* (nmol/g)	Chl *a*/ Chl *b*
WT		1365.51±53.98	405.98±9.45	3.36±0.06
ch1-1	6	983.44±62.20	nd	nd
	15	921.6±37.54	nd	nd
	16	724.66±51.86	nd	nd
Dex2d	6	914.71±36.97	98.16±13.53	9.5±1.74
	15	944.44±66.41	46.51±24.64	26.14±15.08
	16	868.49±31.91	32.45±13.06	29.98±10.95
Dex4d	6	1101.95±64.50	196.05±15.24	5.64±0.41
	15	1024.09±39.19	127.44±58.63	9.76±5.75
	16	964.23±82.79	72.08±8.79	13.55±2.80

Chlorophyll was extracted from fully expanded rosette leave in WT and with / without Dex treated three independent transformants lines. Error bar represents ± SD (n=4).

Table 2. Analysis of hem and LHCs genes expression

	Dex1d	Dex2d	Dex4d
hemA1	1.17	1.69	1.24
hemA2	-1.09	1.05	1.35
Lhcb1	1.3666	1.2042	-1.2201
Lhcb2	1.4071	1.5305	-1.2840
Lhcb3	1.3393	1.5569	-1.5006
Lhcb4	-1.1490	1.0250	-1.3734
Lhcb5	1.4329	1.1448	-1.2243
Lhcb6	1.1393	1.2351	-1.4126
Lhca1	1.0871	1.1995	-1.0791
Lhca2	-1.2069	-1.1251	-1.9839
Lhca3	-1.0914	1.0301	-1.2501
Lhca4	1.0451	1.2279	-1.1000

Total RNA was extracted from fully expanded rosette leaves,

untreated sample was used for control. Agilent microarray (4×44) was used.

Table 3. amount of CP43 and CP1 from Figure 11A

	CP43		CP1	
WT	97%	100%	104%	97%
ch1-1	111%	119%	71%	55%
Dex0.5d	114%	110%	76%	66%
Dex1d	114%	106%	86%	66%
Dex1.5d	113%	99%	81%	66%
Dex2d	124%	100%	87%	62%
Dex3d	118%	96%	91%	60%
Dex4d	128%	96%	103%	66%

Table 4 Primer for transgenic plasmid

atCAO-pENTR4 forward	CAAAAAAGCAGGCTCCACATG AACGCCGCCGTGTTTAGTCCTT
atCAO-pENTR4 reverse	AGAAAGCTGGGTCTAGATTTAG CCGGAGAAAGGTAGTTTATCATCGC

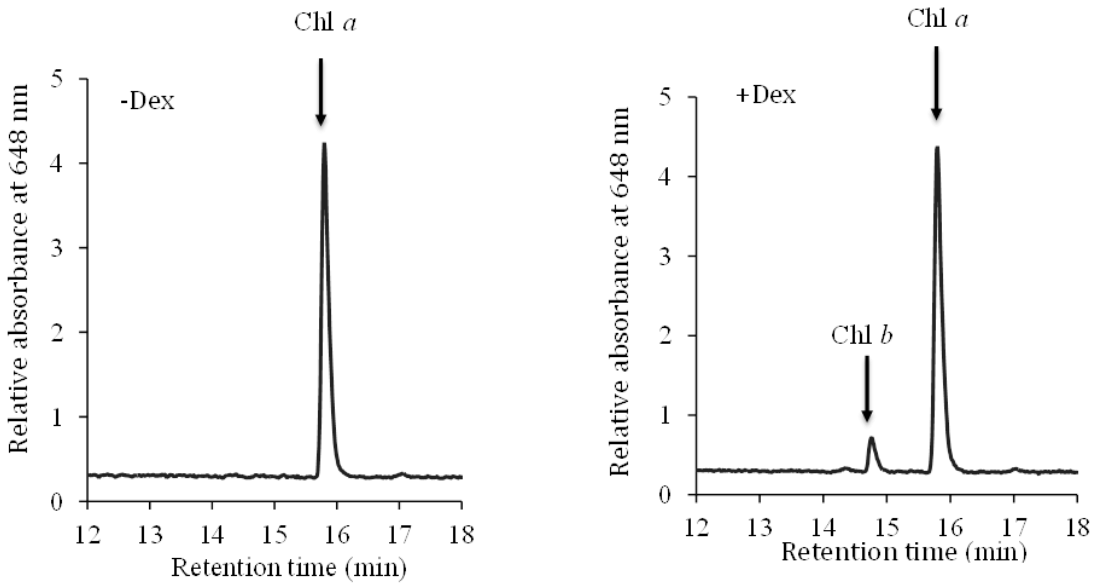

Figure 3. HPLC elution profile of chlorophyll *a* and chlorophyll *b* extract from treated/untreated transformants. Traces were normalized to the peak of chlorophyll *a* at 648nm.

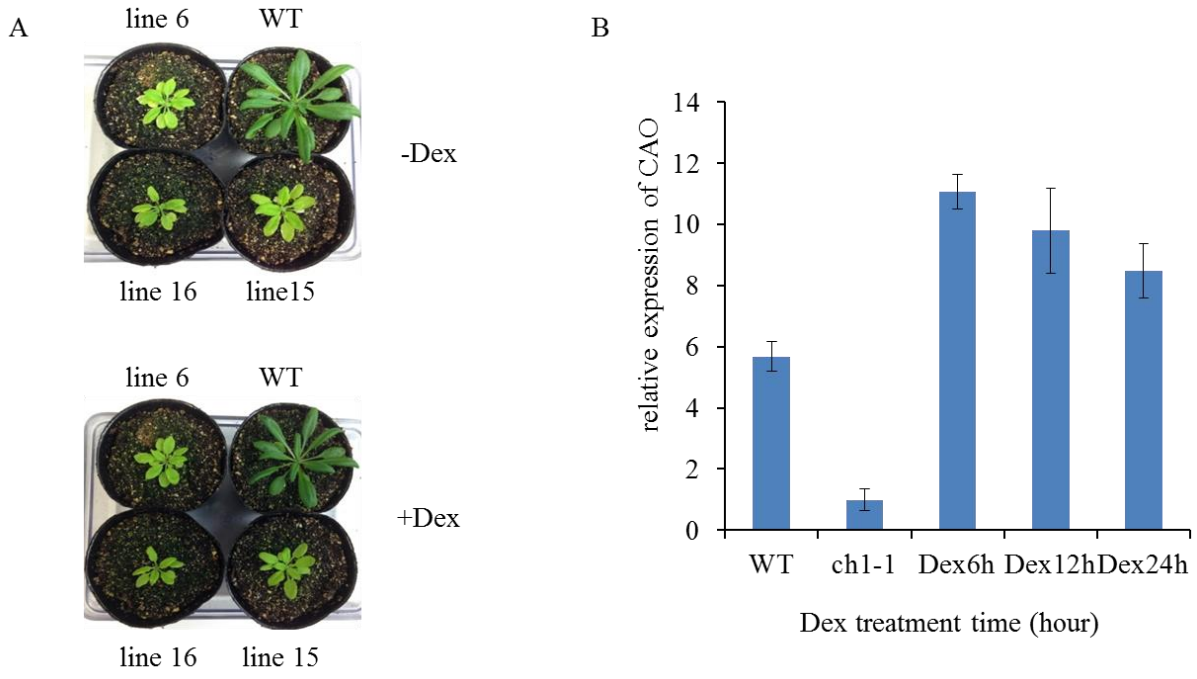

Figure 4. Phenotypic characterization of CAO induction. A, changes in leaf color of three independent lines of CAO over-expressing in *ch1-1* plants before and after Dex treatment. 20μM Dexamethasone (Dex) was even sprayed on the surface of leaves. B, CAO mRNA expression level in 1 day after Dex treatment. transcriptional level of CAO was analyzed by RT-PCR. cDNA was prepared from total RNA which was extracted from fully expanded rosette leaves in line 6. Transcriptional level was normalized using ACT2. Error bar means ±SD (n=4).

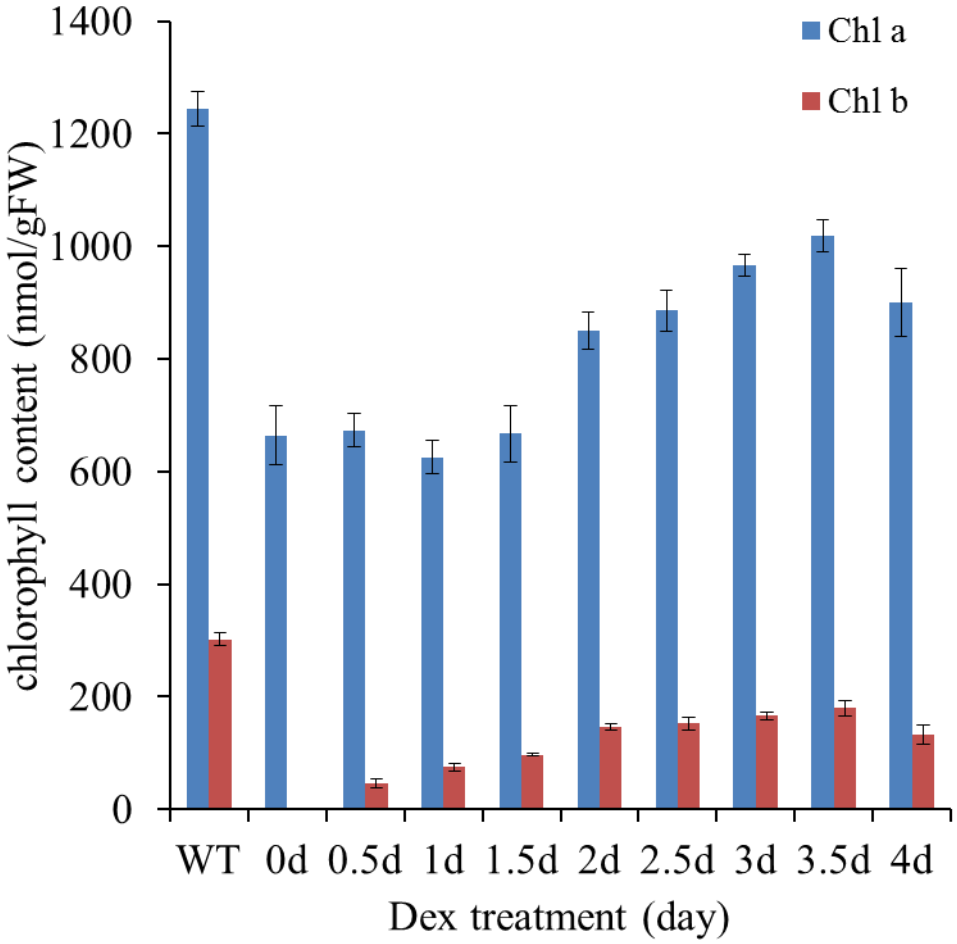

Figure 5. Analysis of chlorophyll content before and after Dex treatment. Chlorophyll was extracted from fully expanded rosette leave in WT (WT) and with / without Dex treated CAO/*ch1-1*. Error bar represents ± SD (n=4).

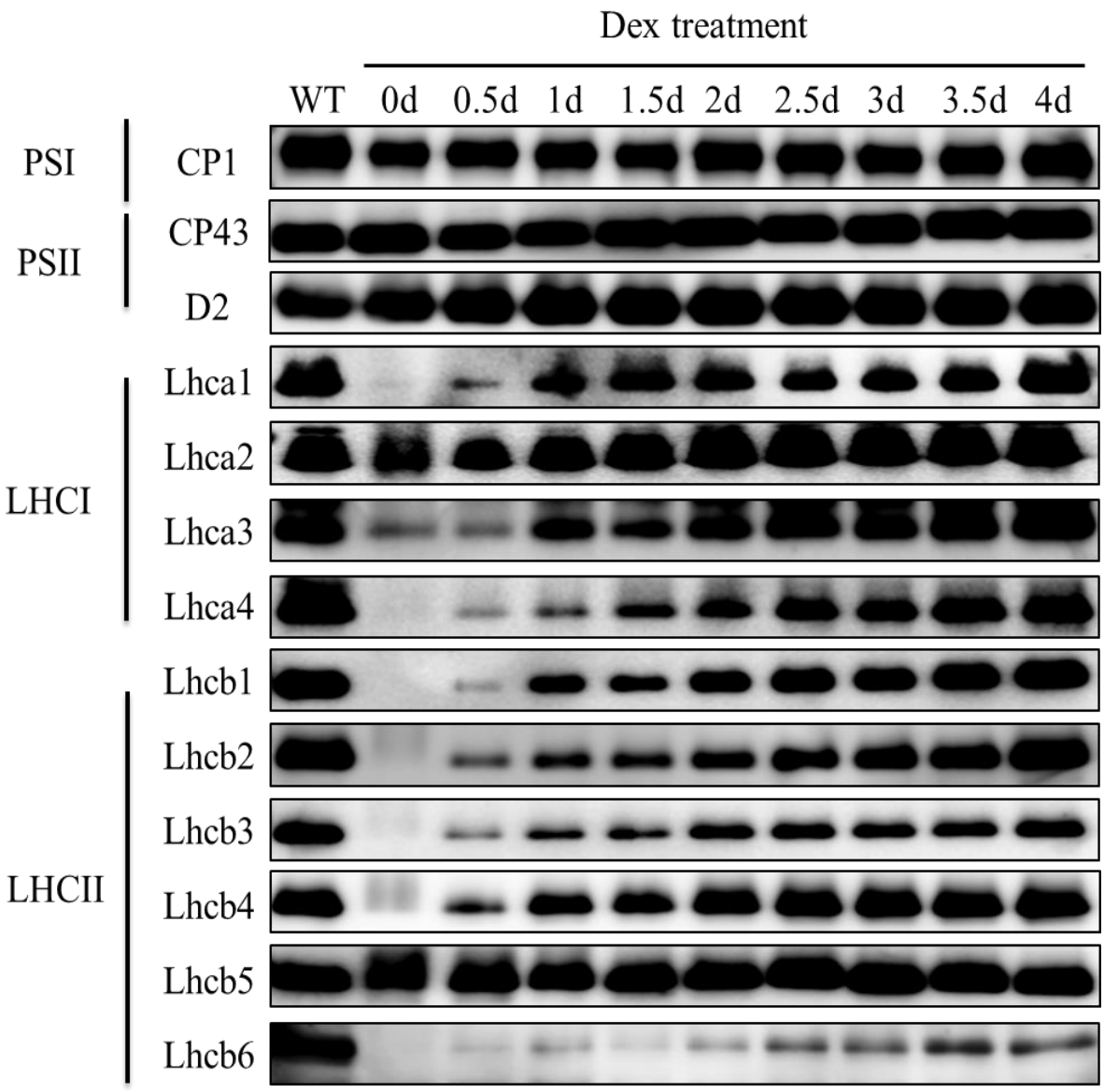

Figure 6. Immunoblotting analysis of LHCs, PSI and PSII core proteins. Total protein was extracted from fully expanded rosette leaves in WT and with/without Dex treated CAO/*ch1-1*. Protein samples were subjected in SDS-PAGE and analyzed. The experiment was repeated three times with similar results. Injection volume was normalized by fresh leaf weight.

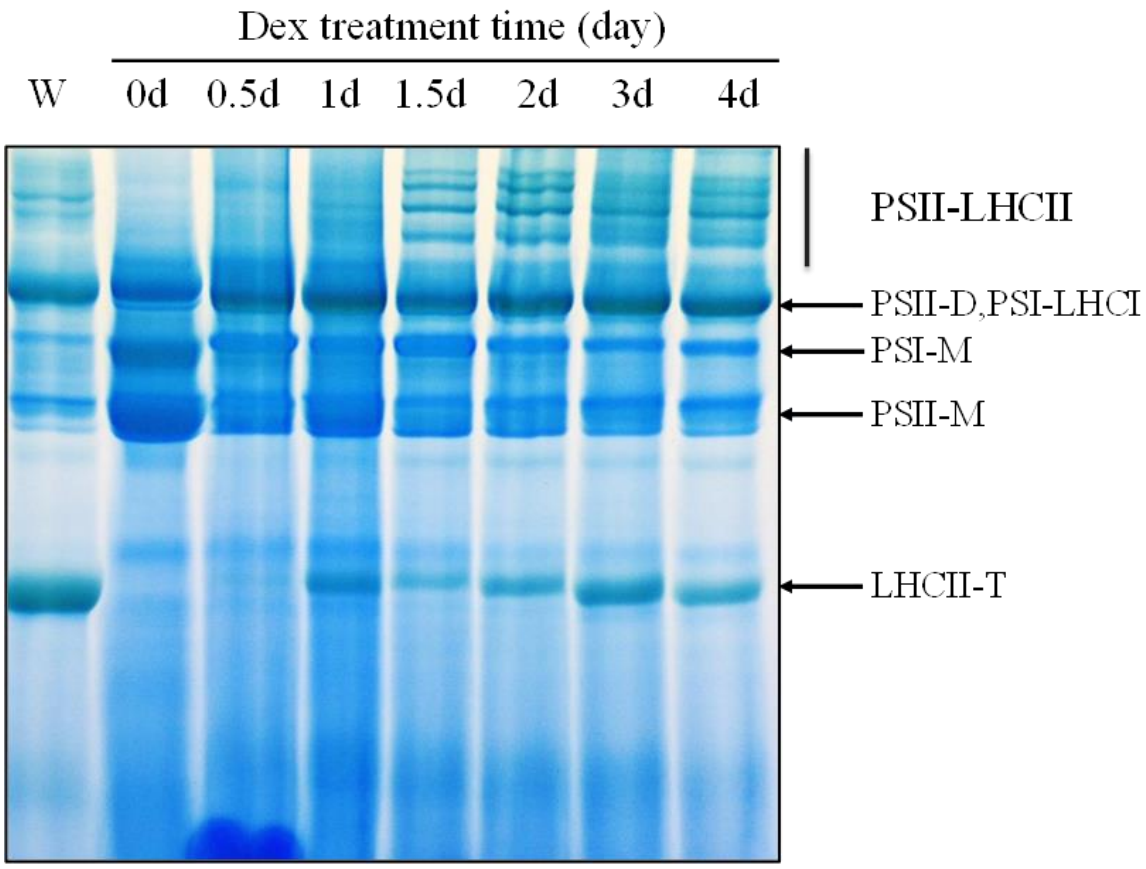

Figure 7. Analysis of protein complexes. Thylakoid membrane containing 4.2 μg chlorophyll was injected in each line, after blue native PAGE, the gel was stained in CBB.

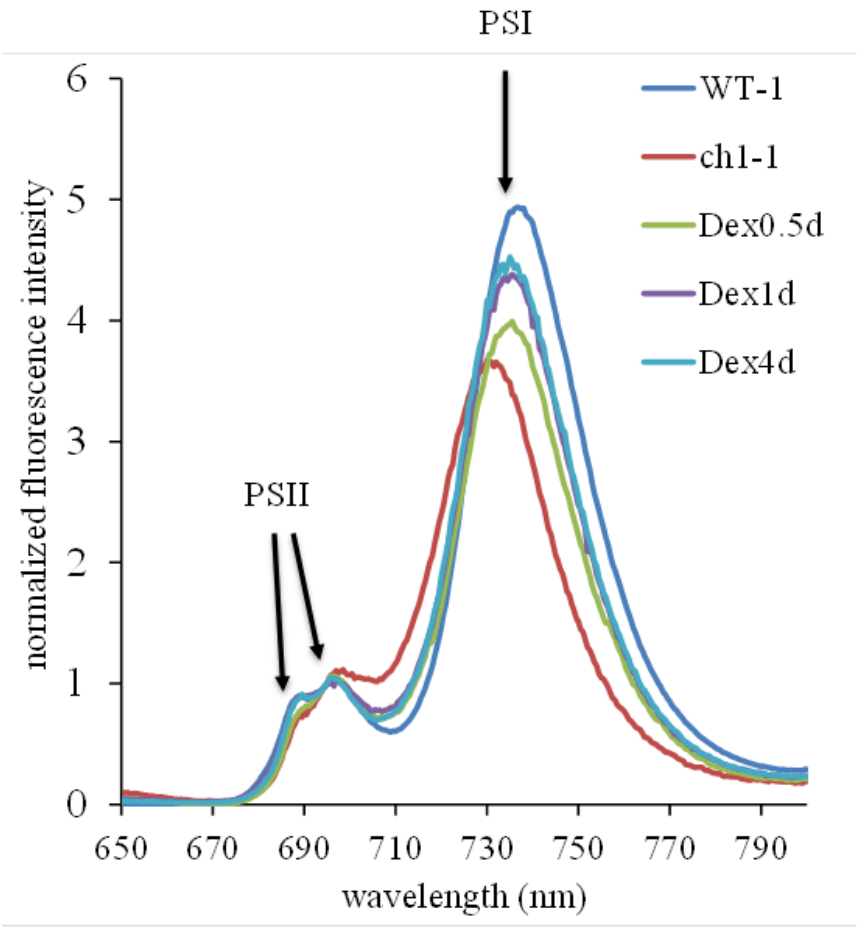

Figure 8. Measurement of low temperature fluorescence. Fluorescence emission spectra were measured with excitation at 465 nm. The curve was normalized at 695nm.

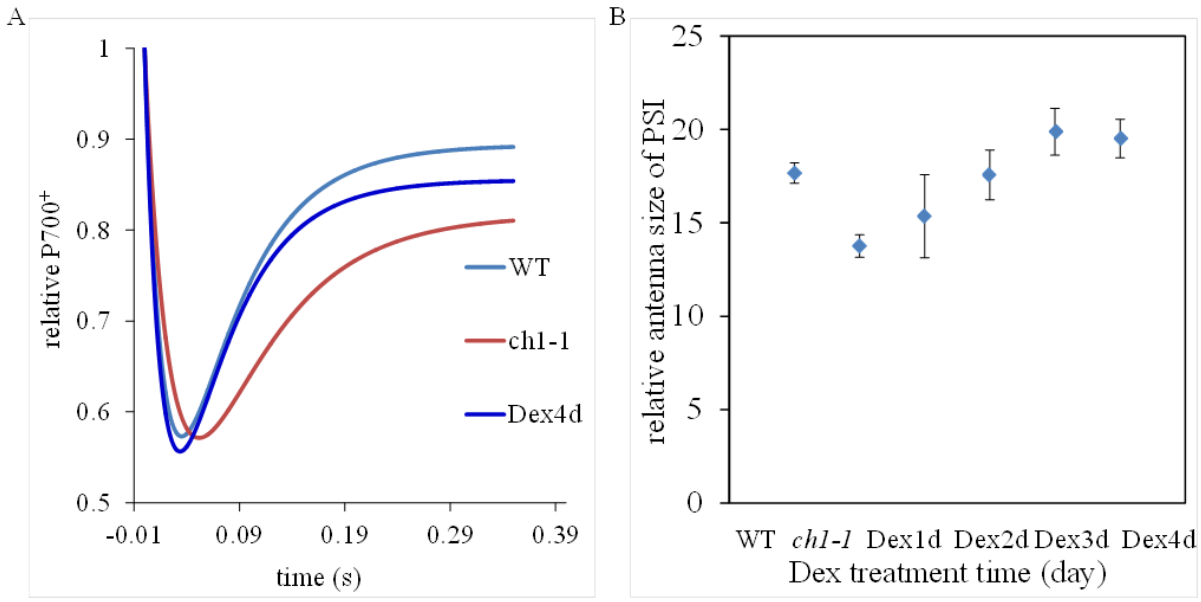

Figure 9. Measurement of functional antenna size of PSI. A, redox changes of $P700^{+}$ was obtained by applying a single turnover flash at 0 sec in steady far red light. B, Co-efficient Kox, which means oxidized P700 indicating by slope of exponent in formula $P700+= \exp(-K_{red}*t)+y_{ss}(1-\exp(-K_{ox}*t))$, was use to indicate relative antenna size of PSI.

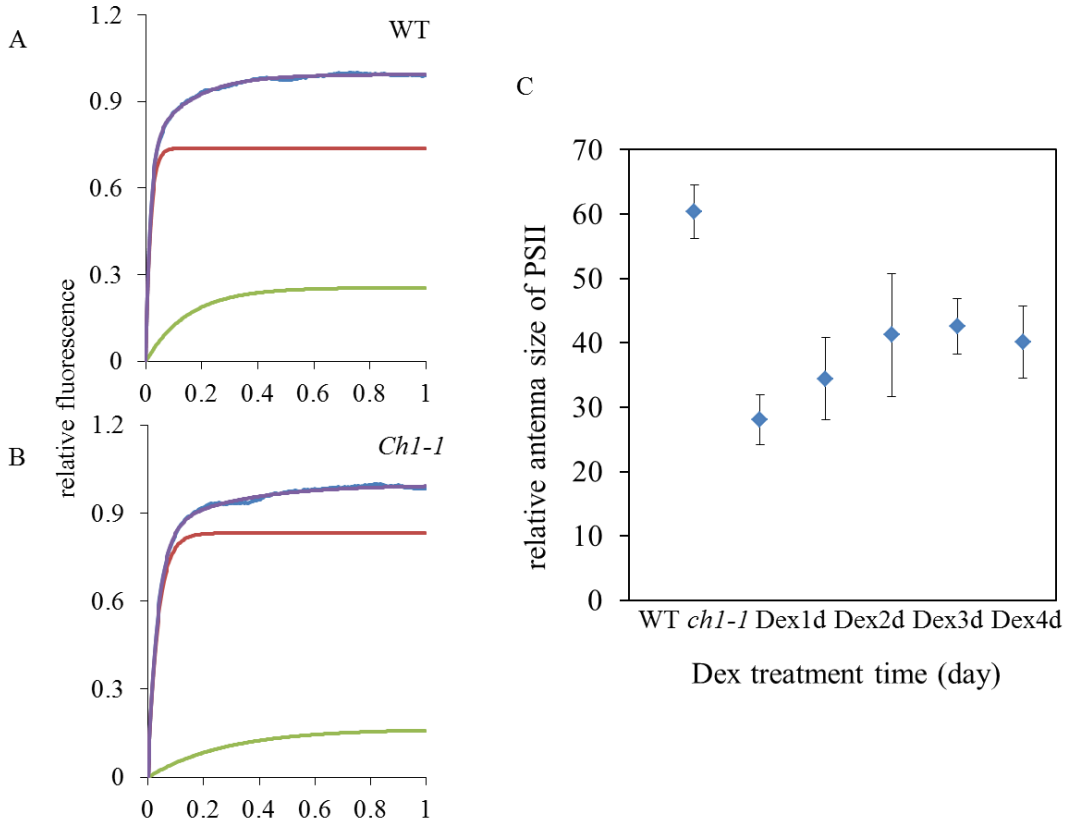

Figure 10. Measurement of functional antenna size of PSII. A and B is kinetics curve of WT and *ch1-1*, C is relative antenna size of PSII. For relative antenna size of PSII, 40 μM DCMU was used to inhibit electron transfer from Q_A to Q_B, photochemical fluorescence in PSII was examined and normalized using the formula: Fv (t) = Kα*Amax*(1 – e-Kα*t)+ Kβ*Bmax*(1 – e-Kβ*t). Blue line is original curve normalized from raw data, purple line is normalized from the formula, red line is α component in kinetics of PSII, green line is β component in kinetics of PSII. Kα , which means slope of α component, was used to indicate relative antenna size of PSII. Error bar represents ± SD (n=4). Independent experiment was repeated three times.

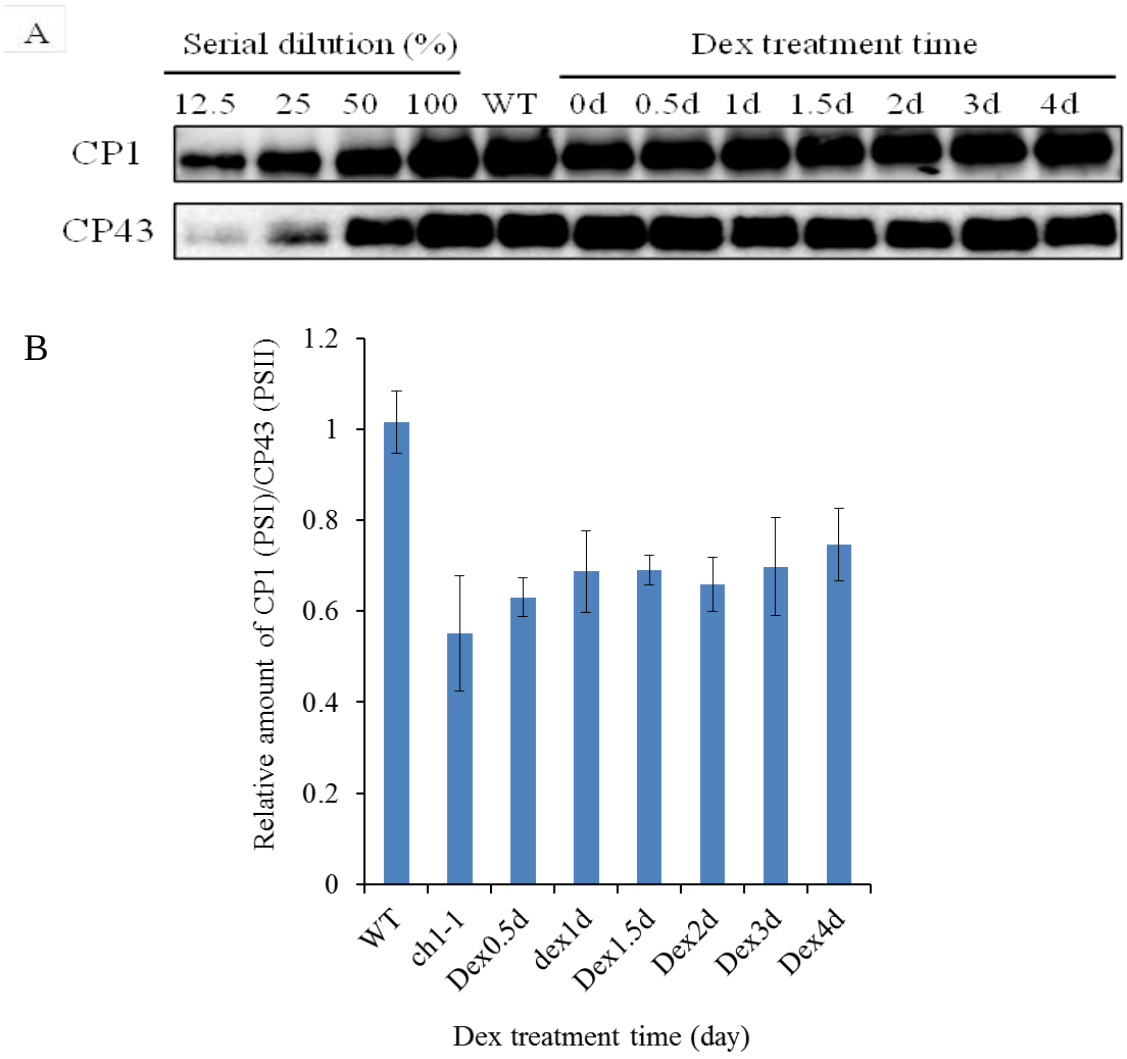

Figure 11. Change of stoichiometry PSI/PSII. A, quantification of CP43 and CP1 protein content. Membrane proteins extracted from leaves were subjected to SDS-PAGE and CP43, CP1 were detected. The sample extracted from WT was used to generate a serial dilution (100, 50, 25 and 12.5%) quantify relative content of CP43 and CP1. B, stoichiometry change of two photosystems. CP1 to CP43 ratio was used to evaluate change of stoichiometry PSII/PSI. Error bar represents ± SD (n=3). Independent experiment was repeated three times.

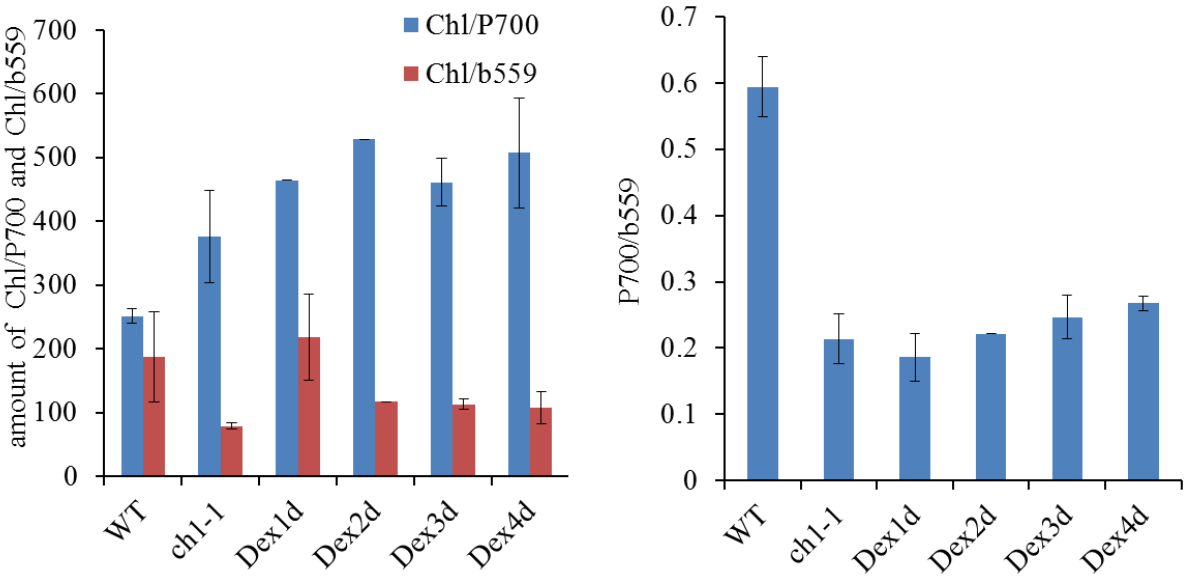

Figure 12. Number of PSI reaction center and PSII reaction center. Thylakoid membrane was separated from fully expanded leaves in WT and with or without Dex treated transformants. The separated particles were wash using 0.2% TrionX-100, then measured at 700nm for Chl/P700, at 559nm for Chl/b559 by specific spectrophotometer. Error bar represents ± SD (n=3). Independent experiment was repeated three times.

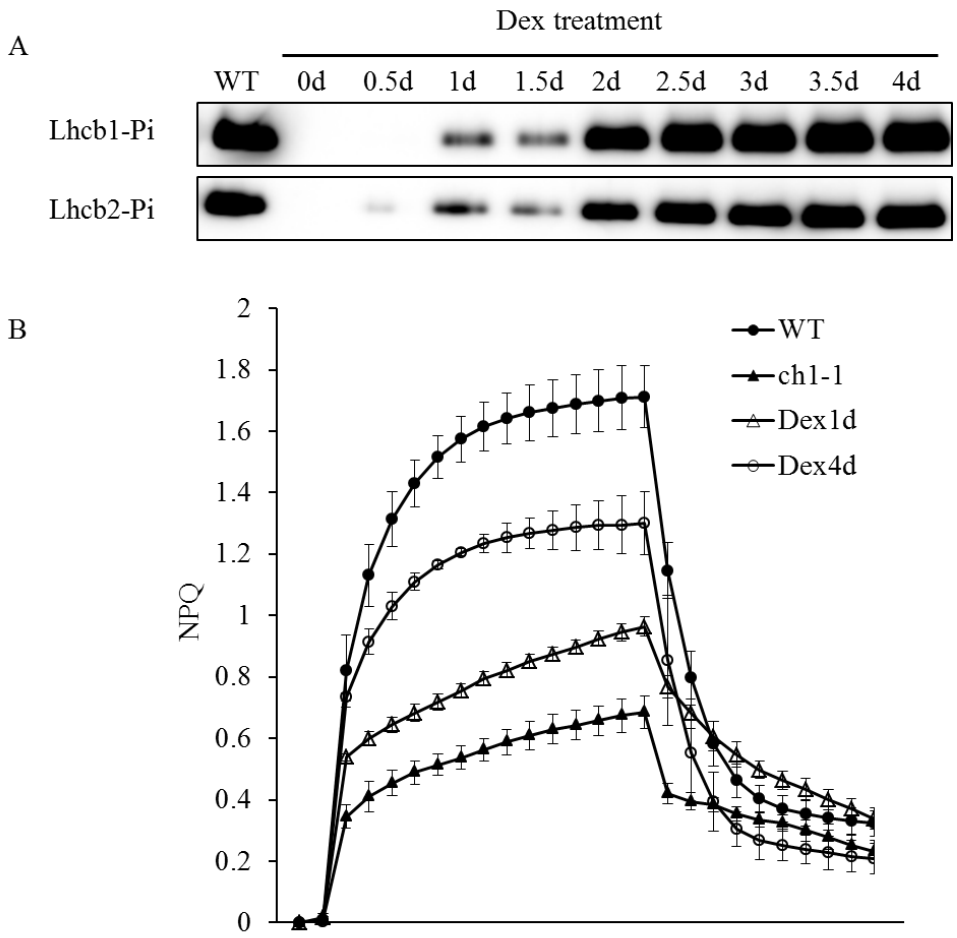

Figure 13 measurement of NPQ and phosphorylated Lhcb1, Lhcb2. A, immunoblotting analysis of phosphorylated Lhcb1 and Lhcb2. Total protein was extracted from fully expanded rosette leaves in WT and with/without Dex treated CAO/*ch1-1*. Protein samples were subjected in SDS-PAGE and analyzed. The experiment was repeated three times with similar results. Injection volume was normalized by fresh leaf weight. B, time course of NPQ. Full expanded leaves from WT and with/without Dex treated transformants were incubated in dark for 15mins, then examined the NPQ using PAM system. Error bar represents ± SD (n=3). Independent experiment was repeated three times.

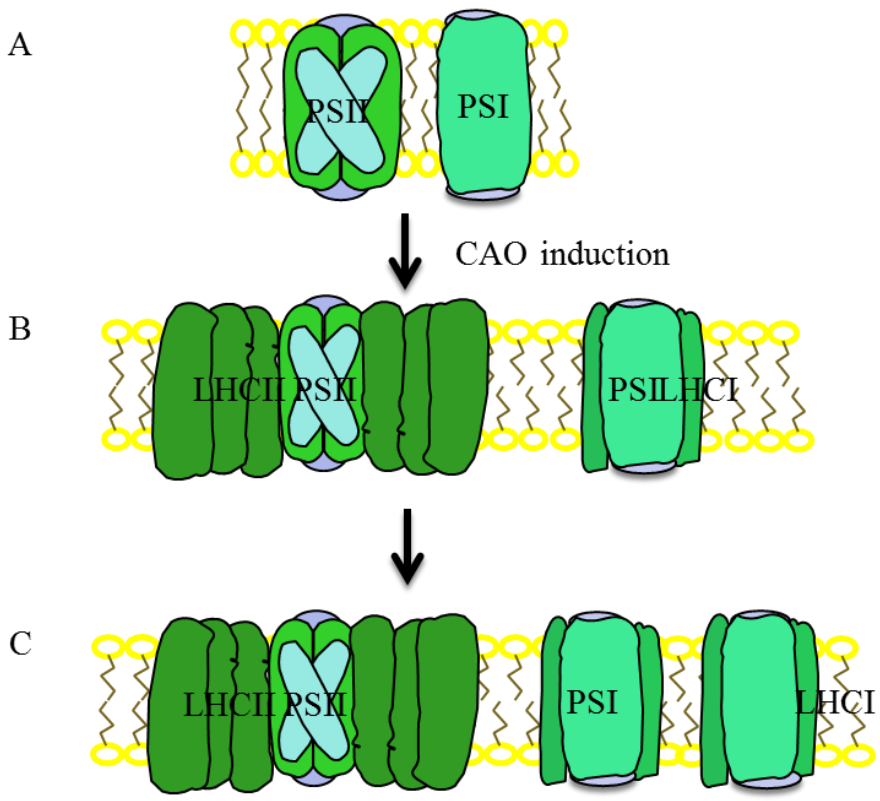

Figure 14. Working model of photosystem I and II after CAO was induced. Energy distribution evenly balance between PSI and PSII in *ch1-1* (A), after CAO induction, LHCs is assembled with PSI and PSII respectively to form peripheral antenna, peripheral antenna size of PSII further larger than that of PSI, this results i n energy distribution imbalance between two photosystems (B). In order to rebalan ce the energy distribution, amount of PSI core increase (C).

Chapter 2 Accumulation of NON-YELLOW COLORING 1 protein of the chlorophyll cycle requires chlorophyll *b* in *Arabidopsis thaliana*

Abstract

Chlorophyll *a* and chlorophyll *b* are interconverted by the chlorophyll cycle. The initial step of chlorophyll *b* to chlorophyll *a* conversion is catalyzed by the chlorophyll *b* reductases NON-YELLOW COLORING 1 (NYC1) and NYC1-like (NOL), which convert chlorophyll *b* to 7-hydroxymethyl chlorophyll *a*. This step is also the first step of the degradation of the light-harvesting chlorophyll *a*/*b* protein complex (LHC). In this study, I examined the effect of chlorophyll *b* on the NYC1 level. NYC1 mRNA and NYC1 proteins were in low abundance in green leaves, but their levels increased in response to dark-induced senescence. When the level of chlorophyll *b* was enhanced by the introduction of a truncated chlorophyllide *a* oxygenase gene and the leaves were incubated in the dark, the NYC1 protein level was greatly increased compared to that of the WT; however, the NYC1 mRNA level was the same as in the WT. In contrast, NYC1 protein did not accumulate in the mutant without chlorophyll *b*, even though the NYC1 mRNA level was high after incubation in the dark. The quantification of the LHC protein showed no strong correlation between the levels of NYC1 and LHC proteins. However, the level of chlorophyll fluorescence of dark adapted plant (Fo) were closely related to the accumulation of NYC1 protein, suggesting that the NYC1 level is related to the energetically uncoupled LHC. These results and previous reports on the degradation of chlorophyllide a oxygenase suggest that the a feedforward and feedback network is included in chlorophyll cycle.

2.1 Introduction

Chlorophyll is a closed tetrapyrrole molecule that plays a central role in photosynthesis. During greening, chlorophyll is actively synthesized and incorporated into proteins to form chlorophyll -protein complexes (61). In contrast, chlorophyll -protein complexes decrease during senescence when chlorophyll and apoproteins are coordinately degraded. In these processes, chlorophyll synthesis and degradation must be strictly regulated (1, 62). If chlorophyll is synthesized in excess, the free chlorophyll will produce reactive oxygen species (63), resulting in cell death. When chlorophyll degradation is not finely regulated, intermediate chlorophyll degradation molecules, such as pheophorbide *a*, accumulate and induce cell death in both a light-dependent (64, 65) and light-independent (66) manner. Chlorophyll metabolism is finely regulated by many factors and environmental conditions at various developmental stages. For example, chlorophyll synthesis is controlled by light via photoreceptors (67) , the redox state (68), temperature (69, 70) and by various environmental stressors (71) . Chlorophyll metabolism is also under the control of phytohormones, such as cytokinin (72). Many translation factors involved in chlorophyll metabolism have been identified (73). Feedback mechanisms and protein factors also contribute to the regulation of chlorophyll synthesis (63, 74, 75).

Green plants contain two chlorophyll species, chlorophyll *a* and chlorophyll *b*, with different absorption spectra. At the last step of chlorophyll synthesis, chlorophyll *a* and chlorophyll *b* are interconverted by the chlorophyll cycle (Figure 2) (76, 77) . Chlorophyllide *a* oxygenase (CAO) is a unique enzyme responsible for chlorophyll *b* synthesis (78, 79). This enzyme converts chlorophyll *a* to chlorophyll *b* via 7-hydroxymethyl chlorophyll *a* (2). Chlorophyll *b* reductase (CBR) converts chlorophyll *b* to 7-hydroxymethyl chlorophyll *a* (76); this is the

first step of chlorophyll *b* to chlorophyll *a* conversion. CBR is encoded by two genes, NON-YELLOW COLORING 1 (NYC1) and NYC1-like (NOL) (3, 80). 7-Hydroxymethyl chlorophyll *a* is then converted to chlorophyll *a* by 7-hydroxymethyl chlorophyll *a* reductase (HCAR) (4). The chlorophyll *b* to chlorophyll *a* conversion has two roles. One is to finely regulate the chlorophyll *a*/*b* ratio. CAO must be regulated to synthesize an adequate amount of *chlorophyll b*. When chlorophyll *b* is over-produced and the chlorophyll *a* to chlorophyll *b* ratio becomes imbalanced, chlorophyll *b* is reconverted to chlorophyll *a*. The chlorophyll *a* is then used for the formation of the inner antenna complexes of PSI and II (chlorophyll recycling) (81, 82). The other function is to degrade chlorophyll *b*. Chlorophyll *b* must be converted to chlorophyll *a* to enter the degradation pathway; the chlorophyll degradation enzyme pheophorbide *a* oxygenase cannot catalyze the ring opening of pheophorbide *b* (83).

The chlorophyll cycle is finely regulated by various mechanisms depending on the environmental condition and the stage of plant development. When green plants are exposed to high light, the CAO mRNA levels immediately decrease. In contrast, CAO mRNA levels gradually increase when plants grown in high light are transferred to low light (36). CAO protein levels are also regulated at a post-translational level (32, 84) with the participation of the Clp protease (84). Chlorophyll *b* to chlorophyll *a* conversion activity was observed during greening where chlorophyll -protein complexes were actively synthesized (76, 82). This activity was also increased during dark-induced senescence (85).

Chlorophyll *a* and chlorophyll *b* differentially locate in the photosystem. Chlorophyll *a* is located in both the inner- and peripheral antenna. In contrast, most chlorophyll *b* is found in peripheral antenna complexes of PSI (LHCI) and PSII (LHCII). It has been suggested that the chlorophyll cycle directly participates in

the formation and degradation of the LHC. The amount of LHCII is related to CAO activity; the LHC is stabilized by chlorophyll *b* (86) and regulated by post-transcriptional mechanisms (87). The conversion of chlorophyll *b* to 7-hyroxymethyl chlorophyll *a* catalyzed by CBR is the first step of LHCII degradation (7). Therefore, LHCII is not degraded in the chlorophyll *b* reductase mutant (*nyc1*) (3). LHC degradation occurs not only during senescence but also during all developmental stages. For example, LHCII degradation activity is high during the early phase of greening when various chlorophyll -protein complexes are actively synthesized (82). It was also reported that the amount of LHCII must be fitted to the light conditions of the environment and that LHCII is degraded under high light conditions (88). LHCII degradation by NYC1 during seed maturation is a crucial process for seed storability (89). These results indicate that the formation and degradation of LHCII is a crucial process at all developmental stages. Questions arise as to how plants distinguish a useless LHC from a functional LHC, and how NYC1 degrades only useless LHC components.

In this study, I investigated the regulation of NYC1 protein levels, which play an essential role in the degradation of the LHC. NYC1 protein did not accumulate in the chlorophyll *b*-less mutant (*ch1-1*) even though NYC1 mRNA was induced as in the WT; this result indicates that chlorophyll *b* is a prerequisite for the accumulation of NYC1 protein. Furthermore, I found that the Fo level is strongly correlated with the accumulation of NYC1 protein. Based on these results, I hypothesize that functionally uncoupled LHCII regulates the accumulation of NYC1 protein.

2.2 Results

2.2.1 The accumulation of the NYC1 protein requires chlorophyll *b*

It is reasonable to assume that the enzymes involved in the chlorophyll cycle are coordinated to finely regulate the chlorophyll *b* levels and to avoid the accumulation of toxic intermediate molecules (7-hydroxymehtyl chlorophyll *a*). To understand the interrelated accumulation of the enzymes of the chlorophyll cycle, I first determined the protein levels of HCAR, NYC1 and NOL when CAO, NOL and HCAR were expressed under the control of the cauliflower mosaic virus 35S promoter. Instead of the full-length CAO protein, a regulatory-domain-deleted CAO fused with GFP (BCG) was overexpressed. This was because the CAO protein level was below the detectable level and because the chlorophyll *b* content was not significantly increased in lines over-expressing the full-length CAO protein due to the feedback suppression by the regulatory domain (32). In this study, the senescence process was induced by a short period (3 days) of dark incubation. BCG plants die after long dark incubation due to the accumulation of pheophorbide *a* (90).

The levels of HCAR, CAO and NOL proteins were successfully increased in their respective over-expressing lines (Figure 15). Overexpression of HCAR and NOL did not induce severe phenotype of green leaves, however, CAO over expressing plants exhibited light green which is consistent to the report that high CAO level was accompanied by the increase in chlorophyll *b* content (32, 91). By using these over-expressing lines, I examined the interrelationships among these enzymes. NYC1 protein in WT plant did not accumulate before dark incubation and increased after dark incubation although the level was low. In WT plants, NOL and HCAR protein levels were approximately the same before and after dark incubation (Figure 16). The accumulation of HCAR protein was not enhanced by the over-production of CAO or NOL. The level of NOL protein accumulation was not affected by the over-expression of CAO and HCAR proteins. Interestingly,

NYC1 protein levels were largely increased in BCG over-expressing plants, especially after dark incubation. The increase in NYC1 protein level was also observed when chlorophyll *b* accumulation was enhanced by introducing *Prochlorothrix hollandica* CAO (Figure 17) (33). A clear band was observed with *ch1-1* mutant although which was slightly smaller than mature NYC1 protein (Figure 15B). The same band was observed with other chlorophyll *b* deficient (*ch1-2*) or chlorophyll *b* less (*ch1-3*) mutant (Figure 18). In order to clarify whether these bands are non-specific bands or truncated NYC1, I examined *ch1-1*/*nyc1* double mutant (Figure 18). In the double mutant, the band did not disappear, indicating that the band is non-specific band. These results clearly indicate that NYC1 protein never accumulated in the chlorophyll *b* less mutant. The total chlorophyll content of BCG plants was slightly lower than that of WT plants before dark incubation and the chlorophyll content was low in the *ch1-1* mutant before and after incubation compared to WT and BCG plants (Figure 15C). The chlorophyll *a*/*b* ratios in WT and BCG over-expressing plants before dark incubation were 3.2 and 1.0, respectively. Chlorophyll *b* was completely missing in the *ch1-1* mutant (Figure 15C). Over 3 days of dark incubation, the chlorophyll content did not significantly change in response to the short dark periods. The immunoblotting results and the chlorophyll measurements suggest that chlorophyll *b* triggers the accumulation of NYC1 protein. One possible mechanism for this accumulation is that the amount of NYC1 mRNA is high in plants that contain high levels of chlorophyll *b*. I compared the NYC1 mRNA levels in WT, BCG and *ch1-1* plants (Figure 19). In WT plants, the NYC1 mRNA level was low before dark incubation; however, the amount of NYC1 mRNA significantly increased after 3 days of dark incubation. The increase in NYC1 mRNA after dark incubation was observed in all mutant lines. It should be noted that the level of NYC1 mRNA was approximately the same in WT and BCG plants. However,

NYC1 protein levels were significantly different. This result suggests that the accumulation of NYC1 protein is post-transcriptionally regulated in response to the presence of chlorophyll *b*. This assumption was also supported by the *ch1-1* mutant. In *ch1-1* plants, the NYC1 mRNA level was high, and the NYC1 protein never accumulated. A comparison of the chlorophyll content and the protein and mRNA levels in these plants indicates that chlorophyll *b* is indispensable for the accumulation of the NYC1 protein. In contrast, NOL protein levels were unchanged after dark incubation and unaffected by the level of chlorophyll *b* in all lines, despite having the same catalytic function.

These results with *ch1-1* and BCG plants indicate the close relationship between CAO and NYC1 protein levels. One possible mechanism for the accumulation of NYC1 is stabilization of NYC1 by forming CAO-NYC1 complex. In order to examine this possibility, I carried out a two-dimensional blue native-PAGE/SDS-PAGE which is one of the powerful tools to examine the protein complexes. CAO form several large complexes corresponding to the trimer and its assembly form as reported previously (92). NYC1 also form a large complex. However, migration distances of CAO and NYC1 were different, indicating that CAO does not form a complex with NYC1 (Figure 20A). Furthermore, endogenous *Arabidopsis* CAO could not be detected when NYC1 accumulated (Figure 20B) as observed in WT (32). CAO might not directly regulate NYC1 level by forming a complex. This assumption is reasonable because NYC1 must increase when chlorophyll *b* synthesis is down regulated during senescence. This conclusion is also supported by the finding that structurally different *Prochlorothrix hollandica* CAO also increased NYC1 level.

2.2.2 NYC1 protein accumulation is correlated with the Fo level

Chlorophyll *b* is indispensable for the accumulation of NYC1 protein. Chlorophyll *b* does not exist as free pigment; rather, most chlorophyll *b* exists as LHC in chloroplasts (93). Taking these facts together, it is reasonable to assume that the LHC causes the accumulation of the NYC1 protein. I examined the relationship between the light-harvesting chlorophyll *a*/*b* binding protein 1 (Lhcb1), a major component of LHCII, and the NYC1 protein (Figure 21). In order to change chlorophyll content and LHC levels, WT, BCG and *ch1-1* plants of different developmental stages were used for the experiments. Although the leaves of different developmental stages exhibited the same color, chlorophyll content per gram fresh weight increased up to 5 weeks and then slightly decreased probably due to the start of senescence (Figure 22). Before dark incubation, WT plants do not accumulate NYC1 protein. NYC1 protein level of BCG plant was 2.7 times larger than that of WT, whereas the LHCII level of BCG plant was larger than that of WT by about 57% in 4-week old plants (Table 5). After dark incubation, NYC1 proteins accumulated in the WT plants; however, the NYC1 protein level in the WT plants was much lower than that observed in the BCG plants, and the LHCII level was not significantly different between the WT and BCG plants. NYC1 levels of 6-week plant were not largely different between before and after dark incubation in BCG plant. The NYC1 protein level was undetectable and LHCII abundance was very low in the *ch1-1* mutants. These results indicate that LHCII is indispensable for the accumulation of NYC1. However, the level of LHCII was not closely correlated with that of NYC1. This result suggests that some other factors regulate the accumulation of NYC1 protein after transcription. NYC1 is responsible for the degradation of chlorophyll *b* and LHCII. For this purpose, NYC1 protein must have high activity against excessively accumulated or damaged LHCII. Under stressful conditions, LHCII might be degraded to avoid further light stress. I examined Fm, Fo, and Fv/Fm and LHC protein levels to

determine which factors were most closely related to the accumulation of NCY1 protein (Figures 23 and 24, Table 5). Leaves from WT, BCG and *ch1-1* plants at various developmental stages were harvested, and NYC1 and LHC protein levels and fluorescence parameters were measured. The NYC1 protein level was not correlated with the LHCII protein level, as supported in Figure 23. Only a weak correlation was found between the NYC1 protein level and Fv/Fm; however, some exceptions were found (Figure 24). This result indicates that damage to the PSII reaction center does not result in NYC1 protein accumulation. Fm levels exhibited no correlation with NYC1 protein levels. But the correlation coefficient between NYC1 protein level and Fo value was significant ($P<0.01$), suggesting that NYC1 protein levels show a strong correlation with Fo values. The origin of Fo is not yet fully understood; energetically uncoupled LHC might contribute to an increase in the Fo level. To know the status of the LHC, the fluorescence spectra of the leaves were measured at liquid nitrogen temperature, and the LHC fluorescence was examined. Fluorescence corresponding to LHCII increased after dark incubation in BCG over-expressing plants (Figure 25). This is consistent with an increase in the Fo level, suggesting the existence of energetically uncoupled LHC in BCG over-expressing plants.

Most of the LHC associates with PSII to form PSII supercomplexes. It has been reported that the attachment and detachment of LHC to PSII is regulated by LHC phosphorylation/dephosphorylation (94). I examined the phosphorylation state of Lhcb1 by immunoblotting (Figure 21). The phosphorylation state of Lhcb1 in BCG over-expressing plants was greater than that in WT plants at all developmental stages. The phosphorylation state of Lhcb1 was partially correlated with the accumulation of NYC1 protein (Figure 23). However, the phosphorylation level of LHC did not increase when WT or BCG over-expressing plants were incubated in

the dark for 3 days, although the NYC1 protein level increased significantly. These results indicate that phosphorylated LHC is not directly related to the accumulation of NYC1 protein.

2.3 Discussion

Chlorophyll *b* reductases catalyze the first step of LHC degradation by converting chlorophyll *b* in the LHC to 7-hydroxymethyl chlorophyll *a*. Two CBRs, NOL and NYC1, function differently in different developmental stages in *Arabidopsis*. The NYC1 protein plays a central role in LHC degradation during leaf senescence (7, 80) and seed maturation (89). The expression of the NYC1 gene is transcriptionally regulated; ABA is involved (89), and the mRNA level increases during senescence. In this report, I demonstrated that the presence of chlorophyll *b* is required for the accumulation of the NYC1 protein. The chlorophyll *b*-null mutant *ch1-1* did not accumulate NYC1 protein despite the induction of NYC1 mRNA during senescence. CAO-over-expressing plants accumulated a large amount of the NYC1 protein, suggesting that CAO directly interacts and stabilizes the NYC1 protein. However, a BN-PAGE analysis did not support this idea. CAO might not directly regulate the NYC1 level by forming a complex. This assumption is reasonable because NYC1 must increase when chlorophyll *b* synthesis is down-regulated during senescence. This conclusion is also supported by the finding that structurally different *Prochlorothrix hollandica* CAO also increases the NYC1 level.

The next question is whether chlorophyll *b* or the LHC controls the accumulation of NYC1. It is likely that chlorophyll *b* does not regulate the stability of NYC1, as all of the chlorophyll *b* binds to proteins in chloroplasts. Most chlorophyll *b* associates with the LHC; it can be hypothesized that the NYC1 protein is stabilized

by binding to the LHC. This observation is supported by the report that chlorophyll *b* reductase has direct access to the LHC (6) and converts its chlorophyll *b* to 7-hydroxymethyl chlorophyll *a* (7). These reports suggest a direct interaction between the NYC1 protein and the LHC. However, this scenario is not plausible; LHC accumulates in sufficient amounts to bind to NYC1 protein at all developmental stages, but the accumulation of the NYC1 protein was largely different depending on the developmental stage of the plant. Indeed, Figure 23 clearly shows that the total amount of LHC and NYC1 protein is not strongly correlated. This observation suggests that the accumulation of NYC1 protein is not determined by the total amount of LHC. It is well known that LHCII localizes differently in thylakoid membranes. For example, some LHCII are assembled at PSII or PSI. The other LHCII exist as an LHCII assembly complex or an LHC aggregate, which is not associated with photosystems (95) . The question arises as to which of the LHC pools triggers the accumulation of NYC1 protein. Interestingly, I found a close correlation between Fo and NYC1 protein accumulation. High Fo is associated with impairment in the photosystem reaction centers, the decreased efficiency of energy transfer and an increase in energetically uncoupled LHC (96, 97). Accumulation of energetically uncoupled LHC in BCG plant was also suggested by measuring time resolved fluorescence spectra. BCG plants had 15-20 ns component at around 680 nm, suggesting the presence of energetically uncoupled LHC (98). I found that when BCG over-expressing plants were incubated in the dark to induce senescence, fluorescence from LHC increased. This result suggests that energetically uncoupled LHC increased during dark incubation. It has also been reported that LHC phosphorylation detaches LHCII from the inner antenna of PSII. However, I could not find any strong correlation between phosphorylation and NYC1 protein accumulation. This result indicates that phosphorylated LHC is not a trigger for NYC1 protein accumulation.

Collectively, it is reasonable to assume that some energetically uncoupled LHC is the trigger for the accumulation of NYC1 protein. From a physiological viewpoint, this mechanism is reasonable; useless LHC (that is energetically uncoupled LHC) must be degraded to avoid photodamage. Then the question arises as to by what mechanisms LHCII stabilizes NYC1. Interestingly, similar but opposite phenomenon was reported with CAO. CAO protein is destabilized by chlorophyll *b* and, therefore, the CAO protein level is under detectable level even by immunoblotting under the presence of chlorophyll *b*. This strict regulation was achieved by the regulatory domain of CAO. It was also elucidated that Clp protease is at least partly responsible for the regulation of CAO protein level (84). Interestingly, comparison of NOL and NYC1 elucidated the extensions of NYC1 protein at both C- and N-terminals. One possible mechanism for the regulation of NYC1accumulation is the cooperation of these extension and some proteases as observed with CAO. Further study is necessary to elucidated this mechanism.

The chlorophyll cycle is multifunctional. It controls the chlorophyll *a*/*b* ratio, LHC degradation and the recycling of chlorophyll molecules. To achieve these different functions, the chlorophyll cycle is strictly regulated by transcriptional (36) and post-transcriptional (32, 84) mechanisms depending on the developmental stage of the plant and the environmental conditions. If CAO loses feedback regulation by the regulatory domain, chlorophyll *b* is accumulated in excess and is incorporated into inner antenna complexes (33). This accumulation and incorporation result in photoinhibition under high light conditions. In contrast, the chlorophyll *b* level decreases and growth is retarded if CAO activity is lowered. If CBR activity is enhanced by transformation, the degradation of chlorophyll *b* is also enhanced (6). If CBR activity is lost, the LHC is not degraded. Therefore, the enzymes in the chlorophyll cycle need to be adjusted to the required levels, otherwise severe

phenotypes appear. This regulation is different from other chlorophyll metabolizing enzymes. For example, transgenic lines over-expressing protoporphyrinogen IX oxidase were phenomenologically indistinguishable from control plants and grew at the same rate (99). In this report, I showed that CAO and NYC1 protein levels respond in an opposite manner to the presence of chlorophyll *b* (Figure 26). Chlorophyll *b* is the product of the CAO enzyme. CAO is regulated by negative feedback by chlorophyll *b* to reduce the CAO protein level. In contrast, chlorophyll *b* is the substrate of NYC1 and is required for the accumulation of NYC1 protein. This feedback and feedforward network in the chlorophyll cycle might be an indispensable mechanism for the monitoring and control of the light-harvesting apparatus.

It should be noted that the NOL and NYC1 genes, both of which encode a chlorophyll *b* reductase, are differently regulated. The expression of the NOL gene is not related to senescence; rather, it is constitutively expressed. The accumulation of the NOL protein in the *ch1-1* mutant, in which the NYC1 protein never accumulated, indicates that the LHC is not required for the accumulation of the NOL protein. This differential regulation of NOL and NYC1 expression suggests that these two chlorophyll *b* reductases have different functions. Considering that NOL is constituently expressed, this protein may be involved in the turnover of the LHC or in scavenging free chlorophyll *b*. In contrast, the NYC1 protein plays an important role when plants undergo developmental transitions and severe stress.

The feedforward regulation of NYC1 by LHC might occur in the chloroplast, as LHC exists exclusively in the chloroplast. However, the molecular mechanism of NYC1 protein accumulation is totally unknown. This lack of knowledge is partly because the exact localization of the NYC1 and NOL proteins remains to be determined, and the proteases involved in the degradation of the NYC1 protein

have not been identified. The structural differences between NOL and NYC1 proteins might provide clues to the molecular mechanism of this regulation. Further study is required to clarify the feedback and feedforward network of the chlorophyll cycle.

2.4 Experimental procedures

2.4.1 Construction and cultivation of transformant plants

For the transformation of *Arabidopsis*, a full-length cDNA of the *Arabidopsis* NOL gene was introduced into the multi-cloning site of a pGreenII vector (100) using the SalI and NotI sites. A full-length cDNA of the *Arabidopsis* HCAR gene was introduced into the Gateway entry vector pENTR4 Dual (Invitrogen) and then introduced into the gateway compatible binary vector pEarleyGate100 (101). Primer sets are listed in Table 6. In all transformants, the transgenes were driven by the cauliflower mosaic virus 35S promoter. The constructs were introduced into Agrobacterium tumefaciens (strain GV3101) and transformed into *Arabidopsis* using a floral dip method (55). Homozygous NOL over-expressing transformants and HCAR over-expressing transformants were screened by kanamycin and glufosinate (Basta) resistance, respectively. Mutant plants were obtained as described previously (4, 7, 35).

2.4.2 Plant materials and growth conditions

Arabidopsis thaliana WT (*Columbia*), BCG (CAO over-expressing) (91), *ch1-1* (CAO deficient mutant), HCAR/*hcar* (HCAR over-expressing in a HCAR-deficient mutant), and NOL/*nol* (NOL over-expressing in NOL-deficient mutant) plants were grown at 25 ℃ under long-day conditions (16 h light/8 h dark) in chambers equipped with white fluorescent lamps at a light intensity of 80 μmol m^{-2}

s^{-1}. Rosette leaves were harvested from plants that were 4 to 6 weeks old. *ch1-1* is a chlorophyll *b*-less mutant that grows slowly; only 6-week-old plants were used for the experiments. Detached leaves were put on distilled water wetted filter paper in a rectangular plate wrapped up in dual tinfoil, put in a box and incubating in permanent darkness for 3 days to induce senescence. All of leaves were collected from fully expanded rosettes.

2.4.3 Analysis of chlorophyll

The fresh weight of the detached leaves before and after dark incubation was measured. The leaves were ground in pure acetone stored at -20 ℃ using a Shake Master (Biomedical Science) grinding apparatus cooled in liquid nitrogen (56). Chlorophyll extracts were centrifuged at 20000 *g* for 10 min at 4 ℃. The pigments were analyzed by HPLC with a Symmetry C8 column (150 mm in length, 4.6 mm in inner diameter) (Waters) according to the method described by Zapata et al. (57). Elution profiles were monitored by measuring the photodiode array (SPD-M10AVP, Shimadzu). The chlorophyll content was quantified as the area of the chromatographic peak. All of detached leaves before and after dark treatment were collected from fully expanded rosettes.

2.4.4 RNA isolation and quantitative real-time PCR (qRT-PCR)

Total RNA was extracted from leaf tissues before and after dark incubation using the RNeasy Mini Kit (Qiagen) according to the manufacturer's instructions. The leaf tissues before and after dark treatment were collected from fully expanded rosettes. The samples were used to synthesize cDNA using the PrimeScriptRT reagent kit with gDNA eraser (TaKaRa) qRT-PCR was performed using a Bio-Rad iQ5 real-time detection system (Bio-Rad). All of the primer pairs used for the expression assays are listed in Table 7. For qRT-PCR, the reaction solution

included 2 μl of the cDNA template (all cDNA templates were diluted 50 times), 1 μl of the forward primer (0.4 μM), 1 μl of the reverse primer (0.4 μM), 12.5 μl of the SYBR Premix Ex Taq II (2) (Takara), and 8.5 μl of sterilized distilled water (total volume of 25 μl). qRT-PCR was performed as follows: 95 ℃ for 3 min, followed by 40 cycles of 95 ℃ for 10 s, 55 ℃ for 30 s, 95 ℃ for 1 min and 55 ℃ for 1min. Primer specificity was confirmed by analyzing the melting curves. The ACT2 gene was used to normalize the relative expression levels of the NYC1 and NOL genes.

2.4.5 SDS-PAGE and immunoblot analysis

Membrane fractions were used for immunoblot analysis to reduce nonspecific bands. To extract membrane proteins, the leaf tissues which were collected from fully expanded rosettes were ground in liquid nitrogen and homogenized with PBS buffer (10 mM Na2HPO4, 1.8 mM KH2PO4, 137 mM NaCl, 2.7 mM KCl, pH 7.4). After centrifugation at 20000 *g* for 10 min, the supernatant was discarded, and the pellet was resuspended with water. After centrifugation, the pellet was solubilized with extraction buffer (125 mM Tris-HCl (pH 6.8), 4% (w/v) SDS, 10% (w/v) sucrose, and 10% (v/v) 2-mercaptoethanol). Ten μl of extraction buffer was used for 1 mg of leaf tissue. An equal volume of sample buffer (50 mM Tris-HCl (pH 6.8), 2 mM EDTA, 10% (w/v) glycerol, 2% SDS, and 6% 2-mercaptoethanol) was added to the mixture. The sample was denatured at 95 ℃ for 5 min, immediately cooled on ice, and then centrifuged at 20000 *g* for 10 min at 4 ℃. Eight μl (for the detection of NYC1, NOL, HCAR and CAO) and 2 μl (for the detection of Lhcb1 and phosphorylated Lhcb1) of supernatant were subjected to SDS-PAGE and then transferred onto a polyvinylidene di-fluoride membrane (Hybond-P, GE-Healthcare). Anti-rabbit primary antibodies against NOL (80) (diluted 1:4000), NYC1 (6) (diluted 1:4000), HCAR (4) (diluted 1:4000), CAO (32) (diluted 1:4000),

LHCII (7) (diluted 1:5000), Lhcb1 (diluted 1:4000) (Agrisera) and phosphorylated Lhcb1 (diluted 1:10,000) (Agrisera) were used for immunoblot analysis. Anti-rabbit IgG linked to horseradish peroxidase (GE-Healthcare) was used as the secondary antibody. Both the primary and secondary antibodies were diluted with Can Get Signal (TOYOBO). The horseradish peroxidase activity was visualized using the Western Lightning Plus-ECL (PerkinElmer) chemiluminescence detection kit according to the manufacturers' protocol. Chemiluminescence was detected using a LumiVision (Aisin). NYC1, Lhcb1 and phosphorylated Lhcb1 were quantified using Image J software (NIH). A serial dilution of an extract from a 5-week-old BCG plant after dark treatment was applied on every blotting analysis and used as a calibration curve to determine the relative content of each protein.

2.4.6 Chlorophyll fluorescence measurements

The maximal photochemical efficiency of PSII was measured using a PAM-2000 fluorometer (Walz) after dark adaptation for 15 min at room temperature. The photochemical efficiency of PSII (Fv/Fm), the minimal level of fluorescence (Fo) with all PSII reaction centers open and the maximal fluorescence (Fm) with all PSII reaction centers closed were measured.

2.5 Tables, figures and legend

Table 5. Chlorophyll fluorescence and protein content

		Fo	Fm	Fv/Fm	Protein content (%)		
					NYC1	P-Lhcb1	Lhcb1
0-day dark	WT-4-week	0.282	1.399	0.798	14.4	18.5	89.8
	BCG-4-week	0.51	1.736	0.706	38.2	51.3	140.9
	WT-5-week	0.321	1.554	0.793	14.4	38.3	100.4
	BCG-5-week	0.53	1.6	0.669	22.3	64.0	158.1
	ch1-1-6-week	0.225	0.963	0.766	12.2	1.9	28.7
	WT-6-week	0.301	1.534	0.804	11.3	24.4	112.7
	BCG-6week	0.636	1.856	0.657	43.4	78.4	171.4
3-day dark	WT-4-week	0.329	1.294	0.746	10.7	20.8	69.2
	BCG-4-week	0.973	1.728	0.437	67.9	47.1	71.9
	WT-5-week	0.421	0.566	0.257	25.0	19.0	73.7
	BCG-5-week	1.191	1.205	0.012	86.2	53.3	93.6
	ch1-1-6-week	0.264	0.421	0.373	2.9	2.8	27.2
	WT-6-week	0.314	1.329	0.764	4.8	20.5	74.2
	BCG-6-week	0.809	1.801	0.551	41.2	87.3	100.6

The chlorophyll fluorescence values and the protein content used in Figures 23 and 24 are listed. P-Lhcb1; phosphorylated Lhcb1.

Table 6. List of qRT-PCR primers

names	Primer sequences
NOL-F	5'-CGCCAAAACCTCACGGTTA-3’
NOL-R	5’-GGAGGCGTCATAGGTTCTCTT-3’
NYC1-F	5’-TTGATGACCAAGGACGGGCGTTA-3’
NYC1-R	5’-GCTTTGTAAGATGATGAAAGCGCA-3’
ACT2-F	5’-CTTGCACCAAGCAGCATGAA-3’
ACT2-R	5’-CCGATCCAGACACTGTACTTCCTT-3’

Table 7. List of primers for over-expression plasmids

names	Primer sequences
NOL-F	5’-AAGTCGACATGGCTACTTGGAGTGGTTTCA-3’
NOL-R	5’-TTGCGGCCGCCTACTCTTCAGTAACATACC-3’
HCAR-F	5’-GCAGGCTCCACCATGATCCAAGTTCAAAAGCAAAAAAATATCTTCT-3’
HCAR-R	5’-TACAAGAAAGCTGGGTCTAGATCACGAGGGAAATAGTTTTGGAT-3’

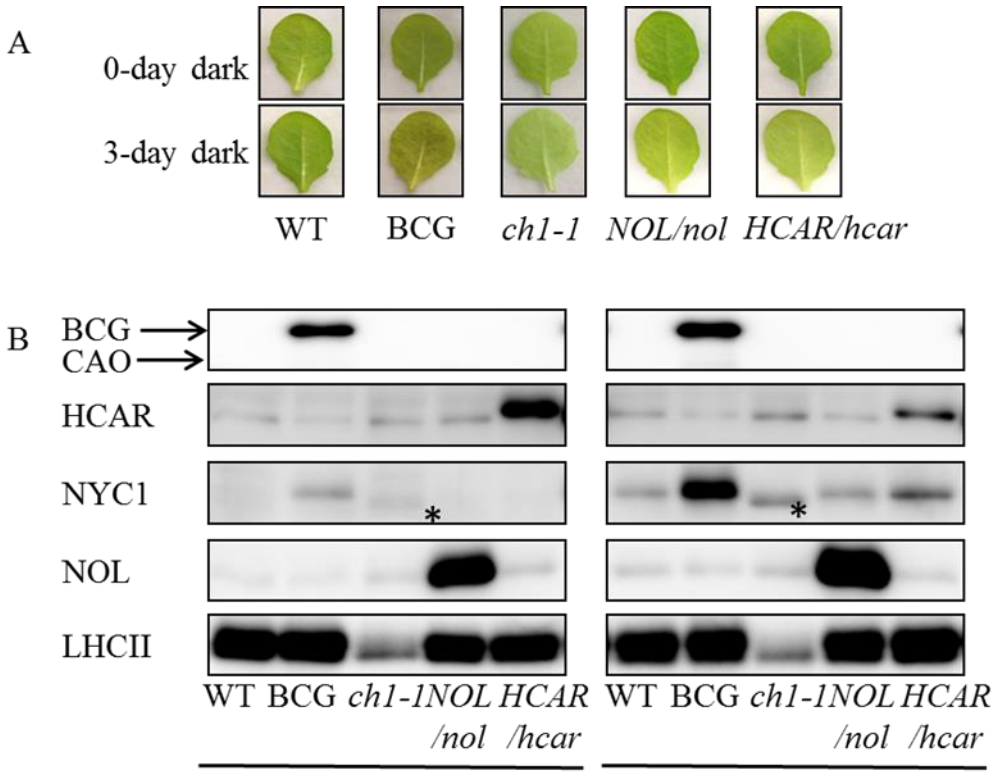
A
0-day dark
3-day dark
WT
BCG
ch1-1
NOL/nol
HCAR/hcar
B
BCG
CAO
HCAR
NYC1
NOL
LHCII
WT BCG ch1-1 NOL/nol HCAR/hcar
WT BCG ch1-1 NOL/nol HCAR/hcar

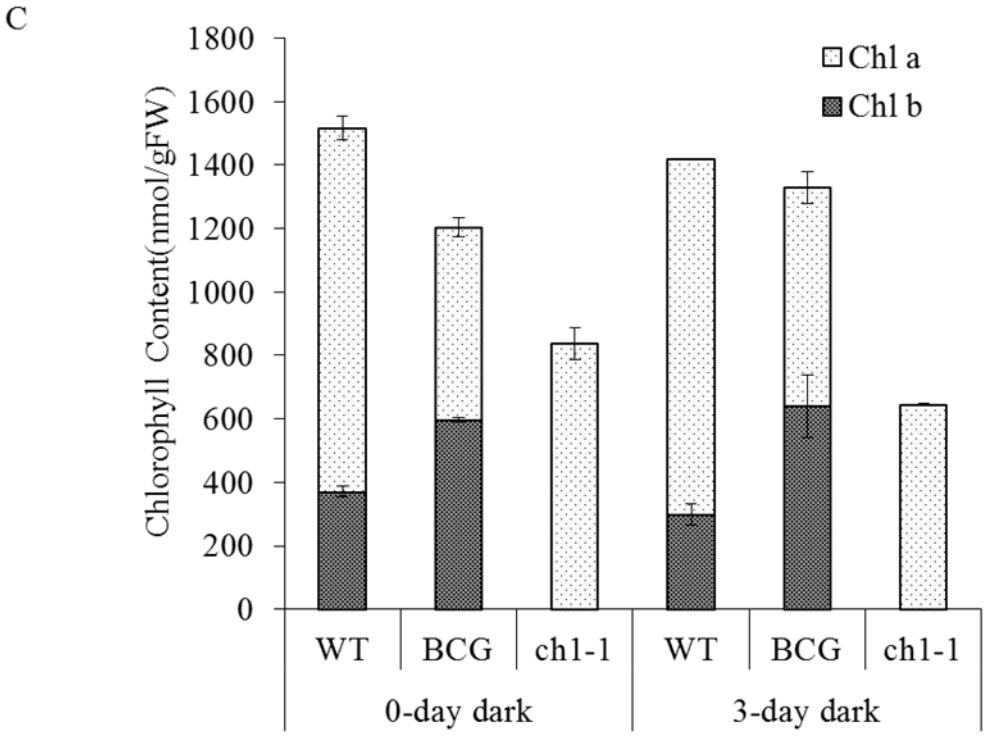
C
Chlorophyll Content(nmol/gFW)
1800
1600
1400
1200
1000
800
600
400
200
0
Chl a
Chl b
WT
BCG
ch1-1
WT
BCG
ch1-1
0-day dark
3-day dark

Figure 15. The effects of CAO and CBR overproduction on chlorophyll content and protein accumulation. A. Leaf color phenotypes during dark incubation. Detached leaves before and after dark senescence from 5-week-old WT, BCG, NOL over-expression in a *nol* mutant (NOL/*nol*) and HCAR over-expression in hcar mutant (HCAR/*hcar*) plants. The leaves from *ch1-1* plants were collected from 6-week-old plants due to slow growth. B. Immunoblot analyses of CAO, HCAR, NYC1, NOL and LHCII proteins. Membrane proteins extracted from leaves were subjected to SDS-PAGE and CAO, HCAR, NYC1 and LHCII proteins were detected. Asterisks represent unspecific proteins reacting to the anti-NYC1 antibody. The full-length CAO (CAO) protein was not detected due to its low abundance. C. Analysis of chlorophyll *a* and *b* contents. Chlorophyll was extracted from the detached leaves of WT, BCG and *ch1-1* plants before and after 3 days of dark senescence and analyzed. Error bars represent ±SD (n=3). Detached leaves before dark senescence were placed on wet filter paper which was wetted by distilled water in a plastic rectangular plate, then the plate was wrapped up in dual tinfoil and incubating in permanent darkness for up to 3 days. All of detached leaves before and after dark treatment were collected from fully expanded rosettes. Double asterisk means highly significant different ($P < 0.01$) by compared with *ch1-1* plants before dark incubation. The difference is not significant ($P > 0.05$) respectively in WT and BCG plants after dark incubation by compared with before dark incubation plants. Student's t test was used for statistical analysis.

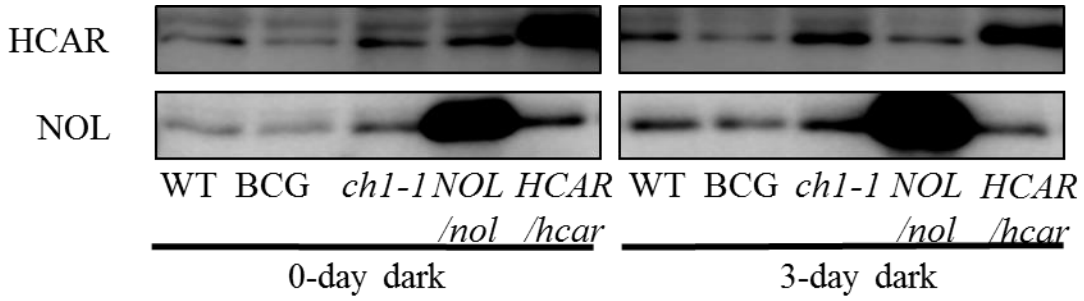

Figure 16. HCAR and NOL levels in plants.

Band intensities in the immunoblotting analysis of Figure 15 were emphasized to compare each bands between the plants. NOL and HCAR levels in the plants having only endogenous NOL and HCAR respectively were similar in those plants.

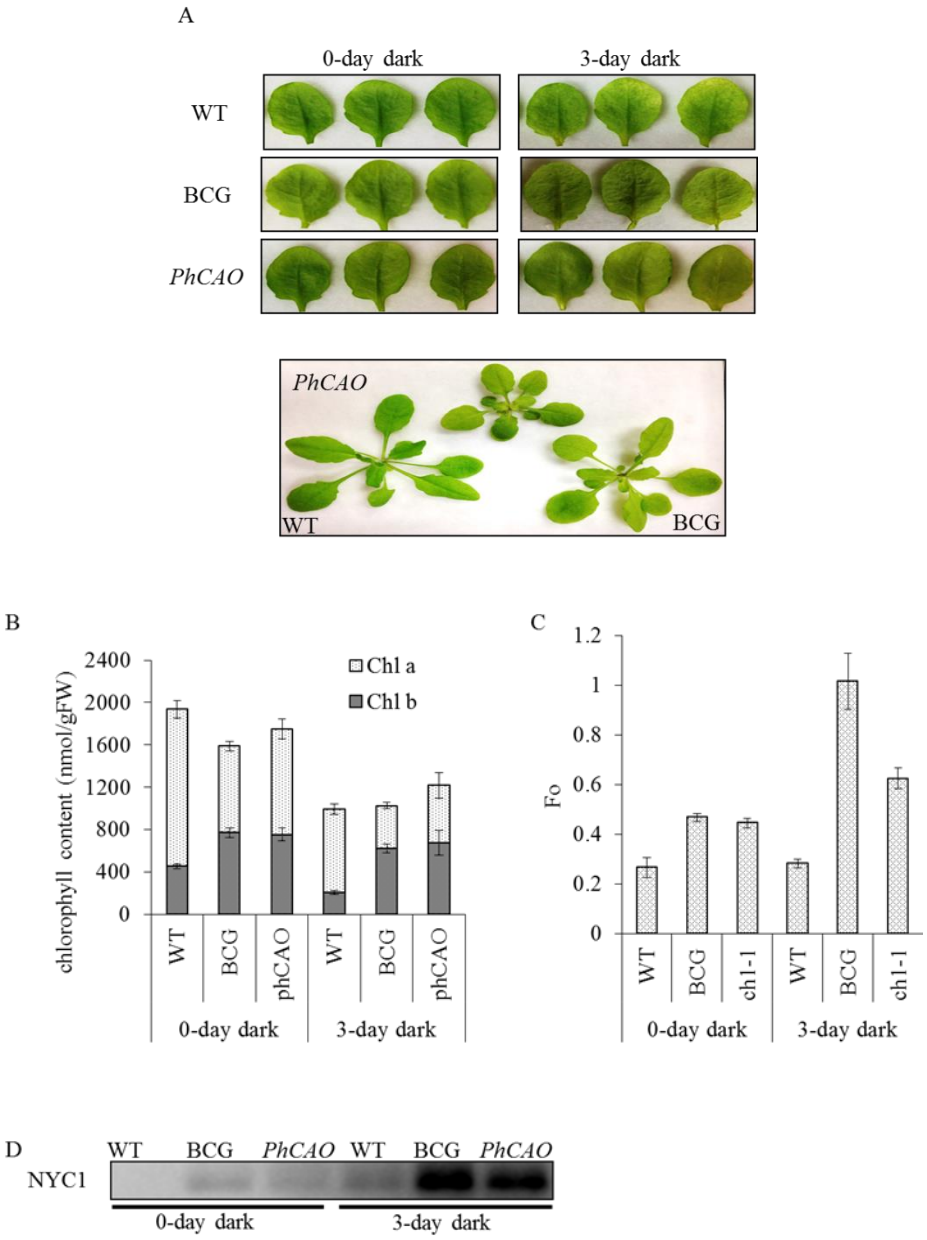

Figure 17. Characteristics of chlorophyll, chlorophyll fluorescence and NYC1 protein in CAO over-expressed plants during dark incubation. A, image of detached leaves and whole plants from 5-week old WT, BCG and PhCAO/*ch1-1* plants. Detached leaves from WT, BCG and PhCAO/*ch1-1* were placed on wet filter paper in a plastic rectangular, then the plate was wrapped up in dual tinfoil and incubated in permanent darkness for up to 3 days. B, analysis of chlorophyll

content. Chlorophyll was extracted from the detached leaves of WT, BCG and PhCAO/*ch1-1* plants and analyzed by HPLC. Error bars represent ±SD (n=3). C, measurement of chlorophyll fluorescence. Minimal fluorescence parameter (Fo) was measured by PAM-2000 after placing the detached leaves under dark condition for 15 minutes. Error bars represent ±SD (n=7). D, Measurement of NYC1 protein level. Membrane proteins extracted from leaves incubated under darkness were subjected to immunoblotting analysis and NYC1 protein was detected. All of detached leaves were collected from fully expanded rosettes.

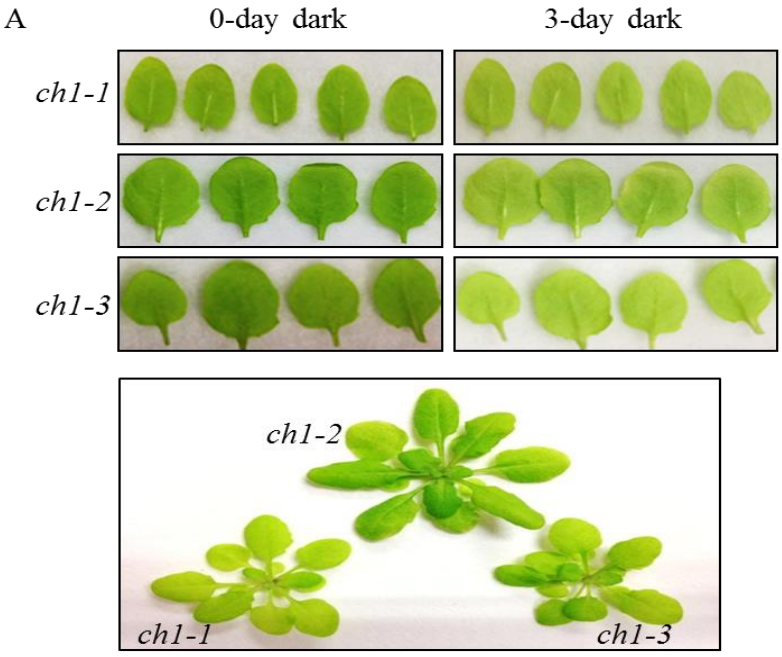
A
0-day dark
3-day dark
ch1-1
ch1-2
ch1-3
ch1-2
ch1-1
ch1-3

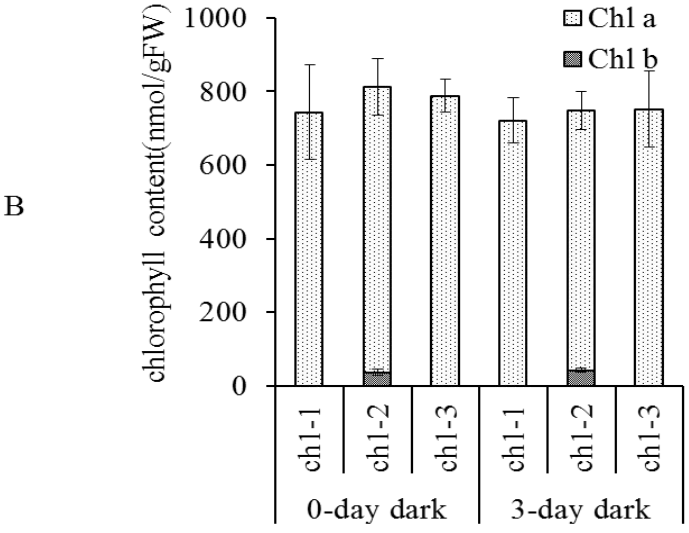
B
chlorophyll content(nmol/gFW)
1000
800
600
400
200
0
Chl a
Chl b
ch1-1
ch1-2
ch1-3
ch1-1
ch1-2
ch1-3
0-day dark
3-day dark

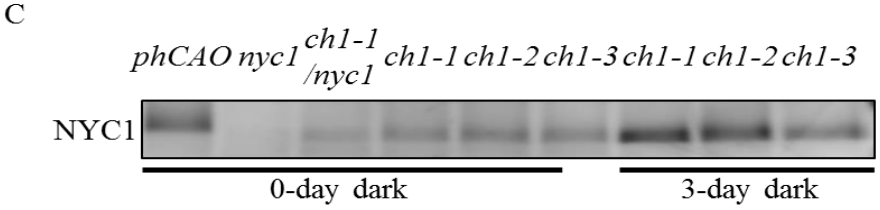
C
phCAO
nyc1
ch1-1 /nyc1
ch1-1
ch1-2
ch1-3
ch1-1
ch1-2
ch1-3
NYC1
0-day dark
3-day dark

Figure 18. Characteristics of chlorophyll and NYC1 protein in *ch1* plants during dark incubation. A. Image of detached leaves and whole plants from 5-week old *ch1-1*, *ch1-2*, *ch1-3* plants. Detached leaves from *ch1-1*, *ch1-2*, *ch1-3* were placed on wet filter paper which was put in a plastic rectangular, then the plate was wrapped up in dual tinfoil and incubated in permanent darkness for up to 3 days. B. Analysis of chlorophyll content in *ch1* plants. Chlorophyll was extracted from the detached leaves of *ch1-1*, *ch1-2*, *ch1-3* plants and analyzed by HPLC. Error bars represent ±SD (n=3). C. Measurement of non-specific band in *ch1* mutant plants. Membrane proteins were extracted from detached leaves and subjecting to immunoblotting analysis. Anti-NYC1 antibody was used to detect NYC1 protein. Lower bands detected in *ch1* plants were also found in *ch1-1*/*nyc1* plants but were not found in *nyc1* deficient plants, suggesting that these lower bands are not NYC1 and specifically accumulated in chlorophyll *b* less or deficient mutant plants. All of detached leaves were collected from fully expanded rosettes.

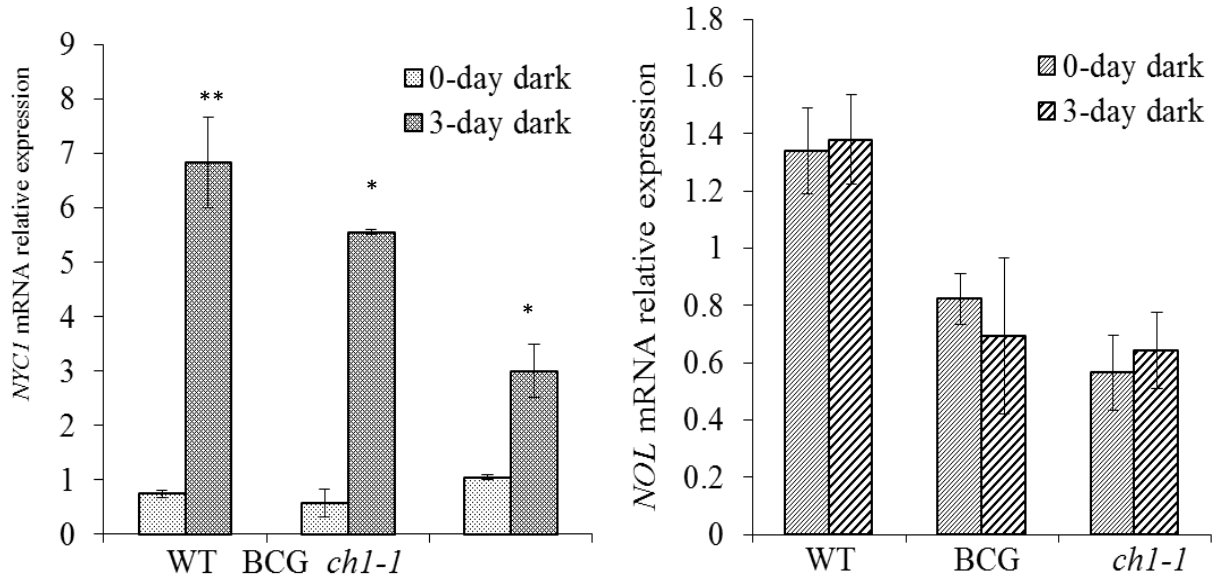

Figure 19. NYC1 and NOL mRNA expression before and after dark treatment. NYC1 and NOL transcripts were analyzed by qRT-PCR. Total mRNA was extracted from leaf tissue from 5-week-old WT and BCG plants and 6-week-old *ch1-1* plants before and after dark incubation. The transcript levels were normalized using ACT2 transcripts. Error bars represent ±SD (n=4). All of leaf tissues before and after dark treatment were collected from fully expanded rosettes. In NYC1 mRNA expression, single asterisk means significant different ($P<0.05$), double asterisk means highly significant different ($P< 0.01$) by respectively compared WT, BCG and *ch1-1* plants after dark incubation with before dark incubation. In NOL mRNA expression, the difference is not significant ($P>0.05$) by respectively compared WT, BCG and *ch1-1* plants after dark incubation with before dark incubation. Student's t test was used for statistical analysis.

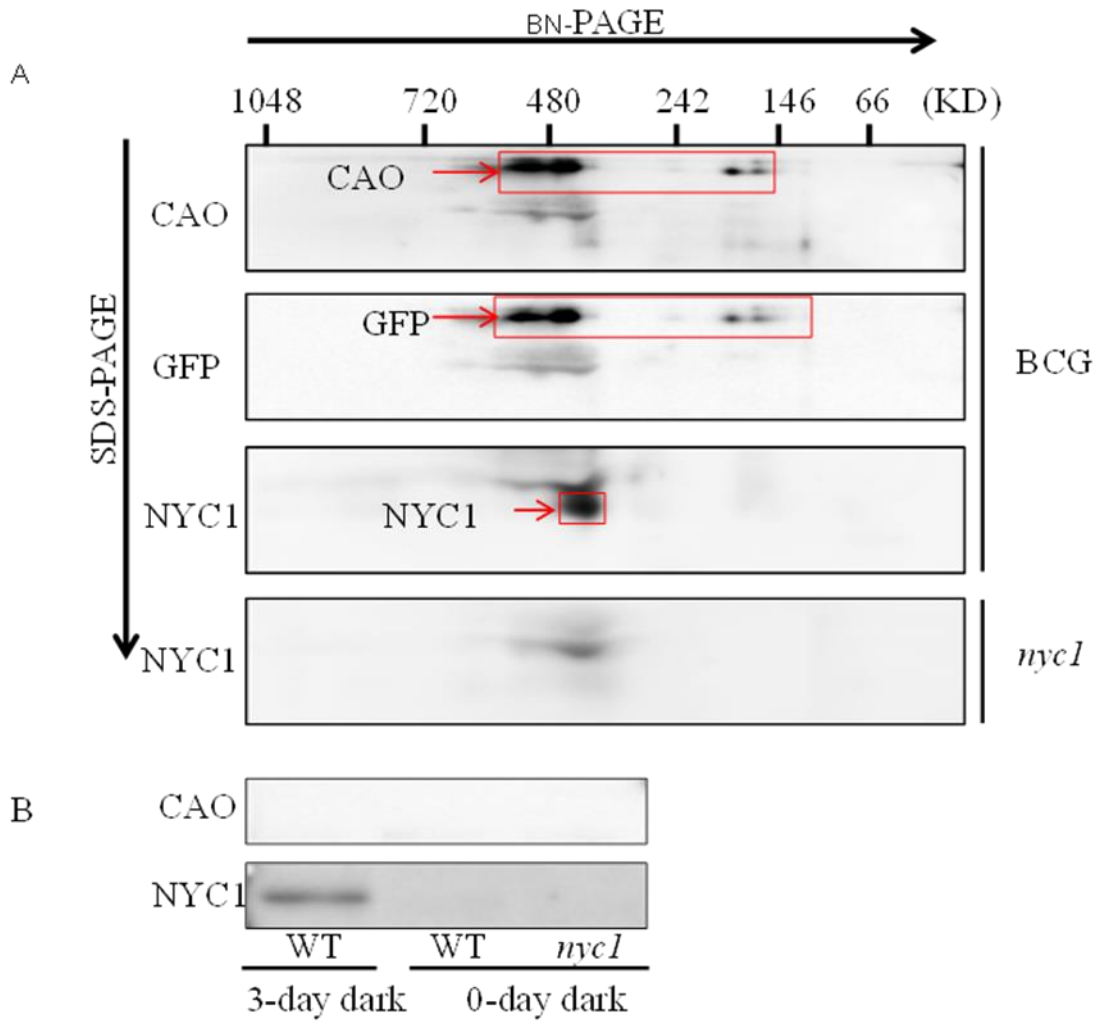

Figure 20. Analysis of protein complexes of CAO and NYC1. A. Accumulation of NYC1 in BCG plants by two-dimensional BN-PAGE/SDS-PAGE. Thylakoid membranes containing 8 μg of chlorophyll were isolated from 3-day dark incubation detached leaves from 5 weeks old BCG and *nyc1* deficient plants respectively. After BN-PAGE, the strips excised from gel were soaked for 1 h at 30℃ in 1% (w/v) SDS solution and run on a second dimension SDS-PAGE. After blotting, anti-CAO, anti-GFP and anti-NYC1 antibodies were used to detect CAO, GFP and NYC1. B Accumulation of CAO in WT plants. Membrane proteins extracted from detached leaves with or without dark treatment of 5-week old WT

and *nyc1* mutant plants were subjected to SDS-PAGE and CAO and NYC1 proteins were examined.

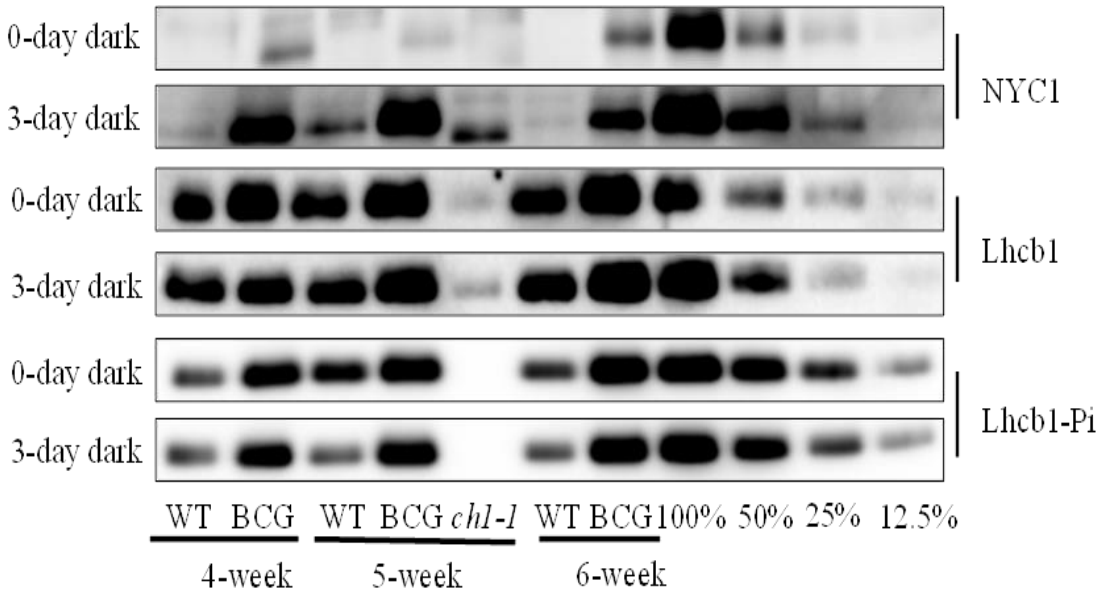

Figure 21. Immunoblot analysis of NYC1, Lhcb1 and phosphorylated Lhcb1 proteins. Membrane proteins extracted from leaves were subjected to SDS-PAGE. NYC1, Lhcb1 and phosphorylated Lhcb1 proteins were detected. The sample extracted from 5-week-old BCG plants after dark incubation was used to make a serial dilution (100%, 50%, 25%, 12.5%) to evaluate the relative content of NYC1, Lhcb1 and Lhcb1-Pi in the samples. The asterisk represents an unspecific protein reacting to the anti-NYC1 antibody. These experiments were repeated three times with similar results. All of detached leaves before and after dark treatment were collected from fully expanded rosettes.

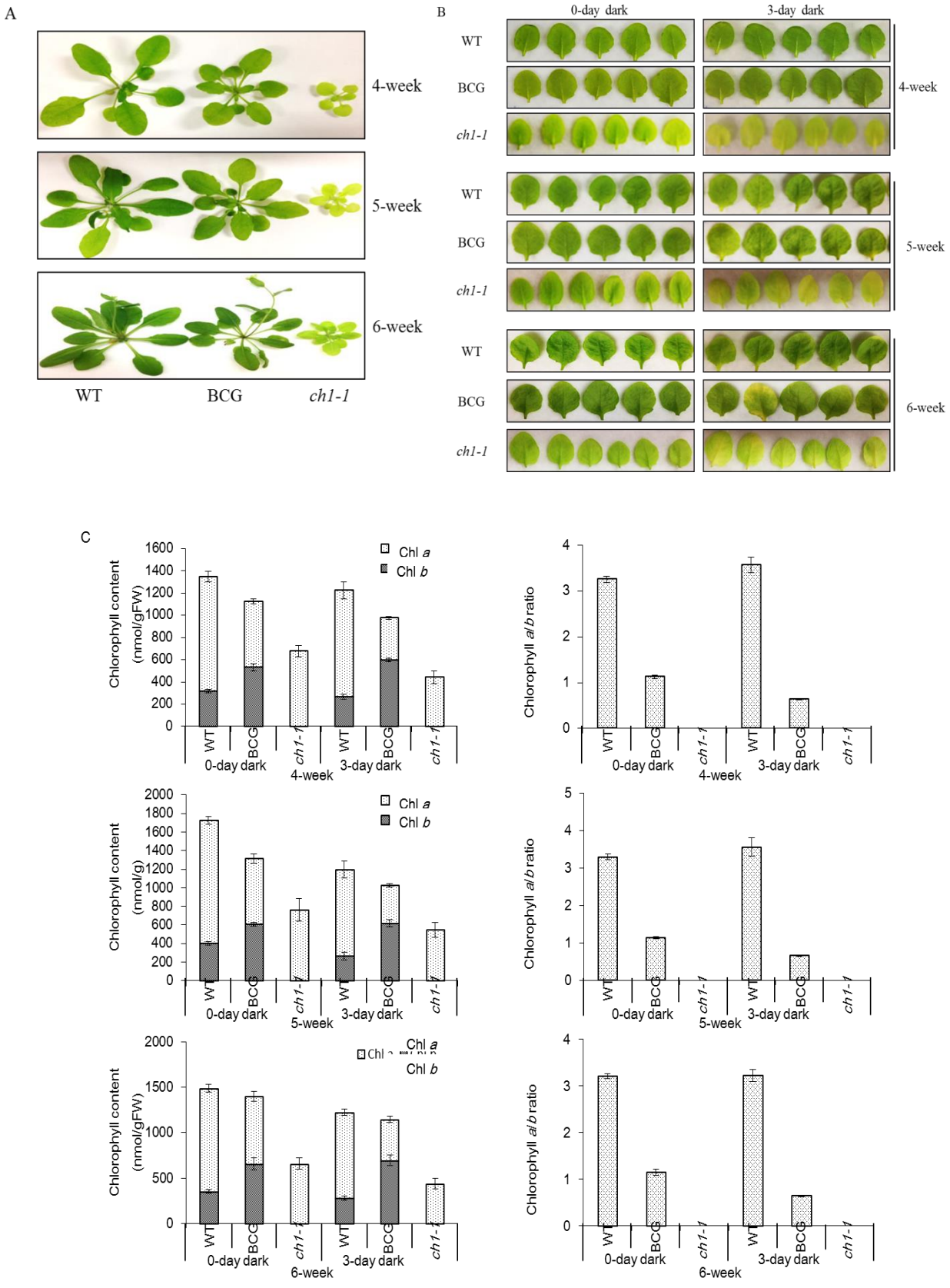
A
4-week
5-week
6-week
WT
BCG
ch1-1
B
0-day dark
3-day dark
WT
BCG
ch1-1
4-week
5-week
6-week
C
Chlorophyll content (nmol/gFW)
Chlorophyll content (nmol/g)
Chlorophyll a/b ratio
Chl a
Chl b
0-day dark
3-day dark
4-week
5-week
6-week

Figure 22. Phenotypes of 4, 5, 6-week old whole plants and detached leaves. A, visible phenotype of WT, BCG and *ch1-1* plants. B, visible phenotype of detached leaves from WT, BCG and *ch1-1* plants before and after dark incubation. Detached leaves before dark senescence from 4, 5, 6-week old WT, BCG, *ch1-1* plants were placed on wet filter in a plastic rectangular plate, then the plate was wrapped up in dual tinfoil and incubating in permanent darkness for up to 3 days. C, analysis of chlorophyll *a* and chlorophyll *b* contents in 4, 5, 6-week old of WT, BCG and *ch1-1* plants during dark incubation. Chlorophyll was extracted from the detached leaves of WT, BCG and *ch1-1* plants before and after 3 days of dark senescence and analyzed by HPLC. Error bars represent ±SD (n=3). All of detached leaves before and after dark treatment were collected from fully expanded rosettes.

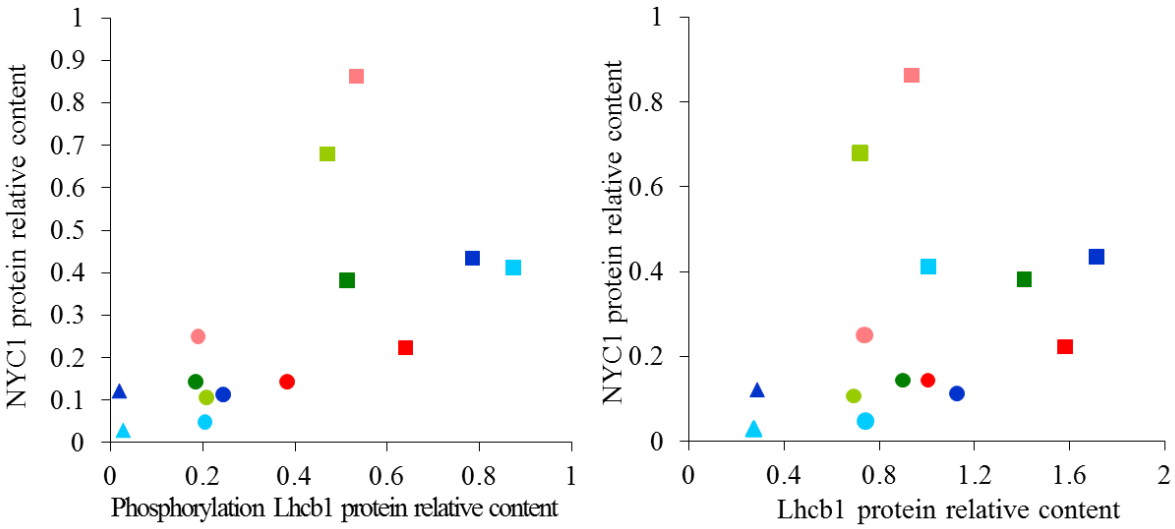

Figure 23. Correlation between the NYC1 protein content and chlorophyll fluorescence. The correlation between the NYC1 content and the phosphorylated Lhcb1 content and the correlation between the NYC1 content and the Lhcb1 content before and after dark treatment were analyzed. The intensity of the band corresponding to NYC1 in Figure 21 was quantified using Image J software. The sample extracted from 5-week-old BCG plants after dark incubation was used to make a serial dilution (100%, 50%, 25%, 12.5%) to evaluate the relative content of each protein in the samples. The values of each point are listed in Table 5. The intensities of the bands corresponding to NYC1, Lhcb1, and Lhcb1-Pi in Figure 21 were quantified using Image J software. The correlation coefficient value between NYC1 protein value and phosphorylated Lhcb1 protein value, Lhcb1 protein value were 0.61 and 0.28, respectively. These experiments were repeated three times with similar results. WT plant (○) , BCG plant ( ), *ch1-1* plant (Δ). 4-week-old, green. 5-week-old, red. 6-week-old, blue. Before dark treatment, deep color. After dark treatment, light color.

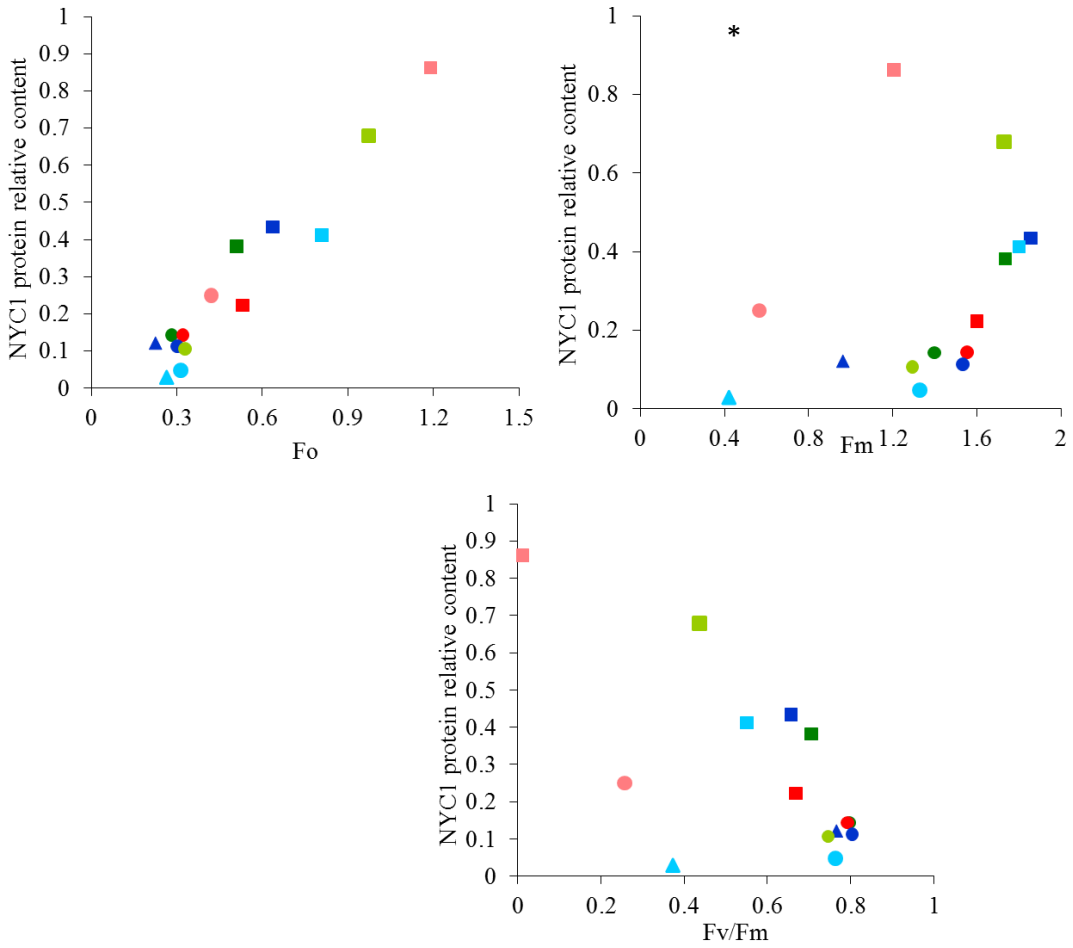

Figure 24. Correlation between the NYC1 protein content and the Lhcb1 protein content. The Fo, Fm, Fv/Fm of detached leaves from WT, BCG and *ch1-1* plants before and after dark senescence for 3 days were measured using a PAM-2000 fluorometer. The correlation between these values and the NYC1 protein content were analyzed. The intensity of the band corresponding to NYC1 in Figure 21 was quantified using Image J software. The sample extracted from 5-week-old BCG plants after dark incubation was used to make a serial dilution (100%, 50%, 25%, 12.5%) to evaluate the relative content of NYC1 in the samples. The correlation coefficient value between NYC1 protein value and Fo, Fm, Fv/Fm values were 0.97, 0.35 and -0.66, respectively. These experiments were repeated three times with similar results. The values of each point are listed in Table 5. WT plant (○) ,

BCG plant ( ), *ch1-1* plant (Δ). 4-week-old, green. 5-week-old, red. 6-week-old, blue. Before dark treatment, deep color. After dark treatment, light color.

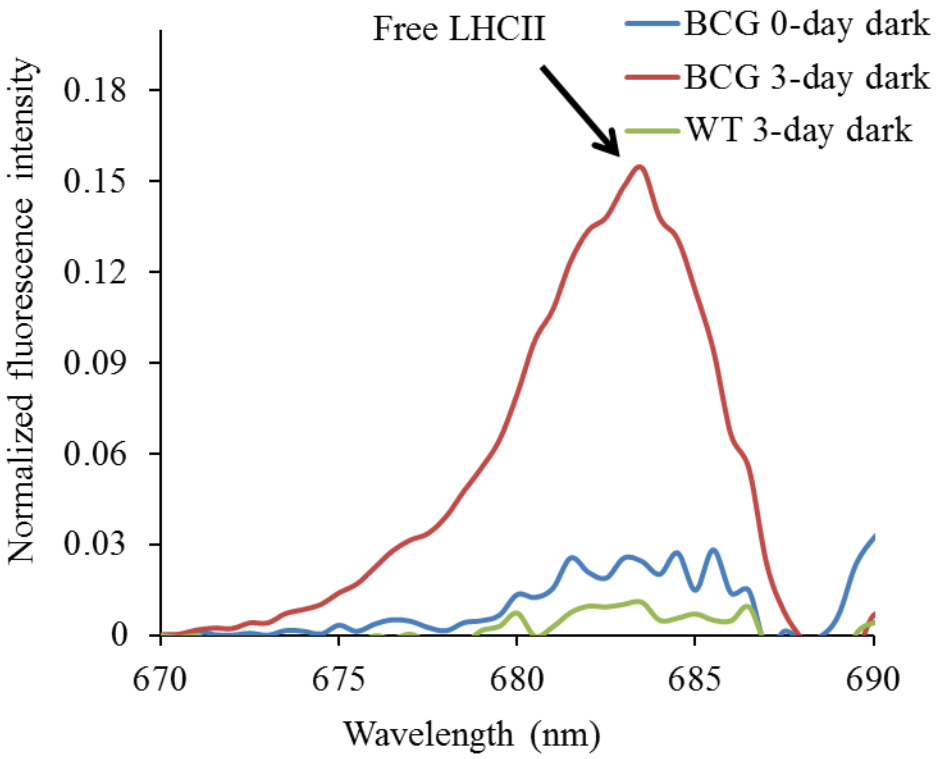

Figure 25. Difference spectra of the low temperature chlorophyll fluorescence. The fluorescence spectra of leaves from WT plants and BCG plants before and after a 3-day dark treatment at 77K were measured. The excitation wavelength was 470 nm. The fluorescence intensities of each sample were normalized to the emission intensity at 670 nm and 687 nm and subtracted from the fluorescence spectrum of the WT plants before dark treatment.

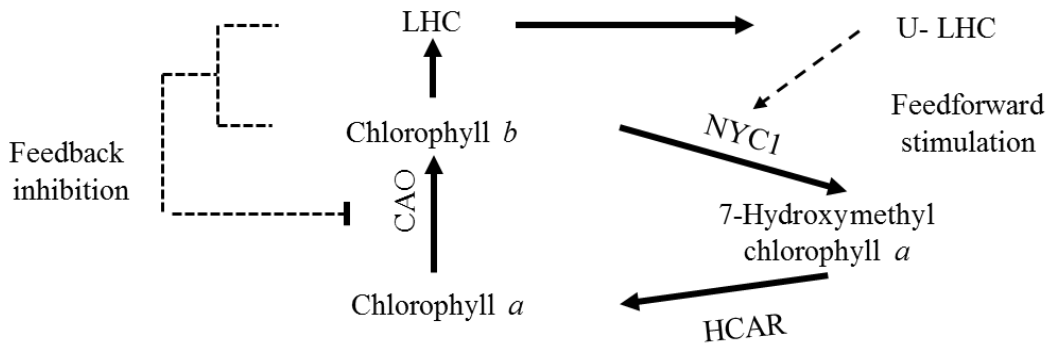

Figure 26. Regulation of the chlorophyll cycle by a feedback and feedforward network. The CAO protein level was negatively regulated by chlorophyll *b* or the LHC. The NYC1 protein level is positively regulated by energetically uncoupled LHC. U-LHC refers to energetically uncoupled LHC. NOL and HCAR are not regulated by chlorophyll *b*. Solid arrows represent the flow of substrate or LHC. Dashed arrows represent the feedback and feedforward regulation.

Chapter 3 The chlorophyll *b* reductase NOL participates in regulating the antenna size of photosystem II in *Arabidopsis thaliana*

Abstract

Chlorophyll exists as chlorophyll–protein complexes in thylakoid membranes. The light-harvesting complexes of photosystem II (LHCII) and CP43/CP47 are the peripheral and core antenna, respectively, of the photosystem. Chlorophyll *b* exists in LHCII but not in the core antenna complex, suggesting that the LHCII level is closely related to the amount of chlorophyll *b*. The first step of the degradation of chlorophyll *b* is catalyzed by chlorophyll *b* reductase (NYC1 and NOL). In this report, we found that the chlorophyll content was significantly lower and that the chlorophyll *a*/*b* ratio was higher in NOL over-expressing *Arabidopsis* thaliana plants than in WT plants. Low temperature fluorescence spectra of the leaves and western blotting analysis revealed that photosystem II had a small antenna size in the NOL over-expressing plants. These results suggest that NOL is involved in the regulation of the antenna size of photosystem II.

3.1 Introduction

Chlorophyll plays a central role in photosynthesis through harvesting light and thereby driving electron transfer and energy production (102). Most chlorophyll exists as chlorophyll-protein complexes, which are located in the thylakoid membrane. Chlorophyll *a* is a component of both the core and the peripheral antenna complexes, whereas chlorophyll *b* only exists in the peripheral antenna complexes. The core antenna contains CP43/CP47 of photosystem II (PSII) and the

P700-chlorophyll *a*-protein complex of photosystem I (PSI). The peripheral antenna includes the light-harvesting complexes of photosystem II (LHCII) (95, 103, 104).

Chlorophyll *b* regulates the photosynthetic antenna size because the antenna size of PSII is determined by the amount of the core and peripheral antenna complexes (42). The LHCII level has been reported to increase when chlorophyll *b* synthesis is enhanced by the addition of 5-aminolevulinic acid (105). In contrast, the LHCII level has been shown to be extremely low in chlorophyll *b*-deficient mutants (106). The degradation of LHCII was not found to occur in rice *nyc1* and *nol* mutants (3) or in *Arabidopsis nyc1* mutants (7) in all of which the chlorophyll *b* level was high even during senescence. Taking these findings together, the amount of LHCII correlates well with the chlorophyll *b* level. This conclusion also indicates that the level of LHCII is not regulated by a protease or by the synthesis of apoproteins but rather by chlorophyll metabolism. In fact, when the chlorophyll *b* synthesis enzyme, chlorophyllide *a* oxygenase (CAO), is over-expressed, the amount of LHCII has been found to increase (36). However, whether chlorophyll *b* reductase participates in regulating the antenna size in green leaves has not experimentally been shown. To address this issue, we over-expressed NOL in *Arabidopsis* and examined the levels of LHCII and chlorophyll *b*, and we found that NOL is involved in the regulation of the antenna size of PSII.

3.2 Results and Discussion

3.2.1 Effect of NOL over-expression on chlorophyll and chlorophyll-binding proteins

To examine the impact of NOL on chlorophyll content, NOL was over-expressed in a *nol* mutant. Figure 1 shows a photograph of the plants before senescence. Interestingly, the old leaves of NOL over-expressing plants were pale green, whereas the young leaves were bright green (Figure 27A). In contrast, all leaves of the WT plant were green regardless of age. To examine whether the NOL and chlorophyll-binding protein levels changed depending on the leaf age, leaves of different ages were classified into three groups (young, middle and old leaves), and their protein levels were determined. Western blotting analyses showed that a large amount of NOL accumulated in the NOL over-expressing plants compared with the WT plants (Figure 27B) and that NOL protein levels were not different among the leaves of different ages. NOL protein levels were also the same among leaves of different ages in the WT plants.

Chlorophyll *b* levels were drastically decreased in the old leaves of the NOL over-expressing plants compared with those of the WT plants and significantly lower in the middle and young leaves (Figure 27C). The chlorophyll *a*/*b* ratios of the leaves of different developmental ages were all approximately 3 in the WT plants; in the NOL over-expressing plants, however, the ratios were approximately 8 in the old leaves and approximately 5 in the middle and young leaves. As previously reported, NOL is a chlorophyll *b* reductase enzyme that can catalyze the first step of the conversion of chlorophyll *b* to chlorophyll *a* (7, 90). The low chlorophyll *b* content and high chlorophyll *a*/*b* ratio in the NOL over-expressing plants indicate that NOL induces a change in the antenna architecture.

Despite leaves of different ages having the same NOL levels in the NOL over-expressing plants, the chlorophyll *a*/*b* ratio differed markedly depending on the age of the leaves, suggesting that the activity of NOL is regulated not only by the NOL

protein level but also by unknown factors, such as NYC1 (3), SGR (107) or certain plant hormones (108).

Next, we compared the levels of the LHCII and CP43 apoproteins in the WT and NOL over-expressing plants. Western blotting analyses (Figure 28) showed that the LHCII apoprotein levels were similar in the leaves of different ages in the WT plants but were lower in the old leaves than in the middle and young leaves in the NOL over-expressing plants. The CP43 apoprotein levels were similar in leaves of all ages in both the WT and the NOL over-expressing plants. These differences are logical because CP43 has no chlorophyll *b* and, therefore, cannot be affected by NOL.

3.2.2 Spectral changes in NOL over-expressing plants

Chlorophyll *b* degradation alters the architecture of the chlorophyll–protein complexes. The architectural changes should be accompanied by changes in the fluorescence characteristics. We measured the fluorescence spectra under liquid nitrogen temperature. Figure 29 shows the fluorescence spectra of leaves normalized to the PSI fluorescence peak. The PSII fluorescence of the NOL over-expressing plants was lower than that of the WT plants, indicating that PSII contains a smaller amount of chlorophyll in the NOL over-expressing plants than the WT plants. Next, we measured the excitation spectra monitored at the emission of PSI and PSII. Excitation peaks were observed at approximately 435 and 465 nm, which correspond to chlorophyll *a* and chlorophyll *b*, respectively. In the NOL over-expressing plants, the excitation peak at 465 nm was lower than that at 435 nm, indicating that chlorophyll *b* levels decreased in the PSII antenna system. Western blotting analyses showed that LHCII levels decreased in NOL over-expressing plants compared with WT plants but that the core antenna did not

change. These results clearly indicate that NOL can regulate the antenna size of PSII by decreasing the level of LHCII associated with PSII.

A previous report suggested that chlorophyll *b* synthesis by CAO controls the level of LHCII (36). Antenna size regulation by CAO might occur at the transcriptional and post-translational levels (32, 106). In addition to CAO, NOL participates in antenna size regulation by degrading LHCII. Collectively, the LHCII level is regulated by chlorophyll *b* synthesis by CAO and by chlorophyll *b* degradation by NOL, both of which might contribute to the fine-tuned regulation of the LHCII level. However, LHCII levels decreased, especially in old leaves, despite the same level of NOL protein being present in NOL over-expressing plants, which suggests that NOL activity is determined not only by the NOL protein level but also by unknown mechanisms.

3.3 Conclusion

In this study, we found that NOL triggers the degradation of LHCII in plant cells, by studying plants that constitutively over-expressed NOL. Together with the degradation of chlorophyll *b*, the antenna size of PSII became smaller. Based on these findings, we conclude that NOL participates in the regulation of the antenna size of PSII.

3.4 Experimental procedures

3.4.1 Plant materials and growth conditions

For NOL transformant, a full length cDNA of *Arabidopsis* NOL was introduced into the multicloning site of a pGreenII vector at SalI and NotI sites. The transgenes were driven by cauliflower mosaic virus 35S promoter. The construct

was introduced into Agrobacterium tumefaciens (strain GV3101) and transformed into *Arabidopsis* through a floral dipping method. Homozygous NOL over-expressing transformants were screened by kanamycin.

Arabidopsis thaliana WT (*Columbia*), and NOL/*nol* (NOL over-expression in NOL-deficient mutant) plants were grown at 25 ℃ under long-day conditions (16 h light/8 h dark) in chambers equipped with white fluorescent lamps at a light intensity of 80 μmol m^{-2} s^{-1}. Rosette leaves in different sites of plants were harvested. The plants were 3-4 weeks old.

3.4.2 Chlorophyll analysis

The leaves were cut and their weights were measured. Then the leaves were ground in cold acetone stored at -20 ℃ using a Shake Master (Biomedical Science) whose grinding apparatus was pre-cooled in liquid nitrogen. The homogenates were centrifuged at 20000 *g* for 10 min at 4 ℃. The pigments were analyzed by HPLC with a Symmetry C8 column (150 mm in length, 4.6 mm in inner diameter) (Waters) according to the method described by Zapata et al. (57). Elution profiles were monitored by measuring the absorbance (SPD-10AV, Shimadzu). The chlorophyll content was quantified as the area of the chromatographic peak.

3.4.3 SDS-PAGE and western blotting analysis

The leaf tissues were ground in liquid nitrogen and homogenized with extraction buffer (125 mM Tris-HCl (pH 6.8), 4% (w/v) SDS, 10% (w/v) sucrose, and 10% (v/v) 2-mercaptoethanol). Ten microliters of extraction buffer was used for 1 mg of leaf tissue. An equal volume of sample buffer (50 mM Tris-HCl (pH 6.8), 2 mM EDTA, 10% (w/v) glycerol, 2% SDS, and 6% 2-mercaptoethanol) was added to the mixture. The sample was denatured at 95 ℃ for 5 min, immediately cooled on ice,

and then centrifuged at 20000 *g* for 10 min at 4 ℃. Six microliters (for the detection NOL) and 1 μl (for the detection of LHCII and CP43) of the supernatant were subjected to SDS-PAGE and then transferred onto a polyvinylidene di-fluoride membrane (Hybond-P, GE-Healthcare,). Anti-rabbit primary antibodies against NOL, LHCII (7), and CP43 (Agrisera) were used for western blotting analysis. Anti-rabbit IgG linked to horseradish peroxidase (GE-Healthcare) was used as the secondary antibody. Both the primary and secondary antibodies were diluted with Can Get Signal (TOYOBO). The horseradish peroxidase activity was visualized using the Western Lightning Plus-ECL (PerkinElmer) chemiluminescence detection kit according to the manufacturers' protocol. Chemiluminescence was detected using a LumiVision (Aisin).

3.4.4 Low temperature fluorescence measurement

Leaves were put into the glass tube for fluorescence measurement and immediately frozen in liquid nitrogen. Fluorescence emission spectra were obtained at 77 K by using fluorescence spectrophotometer (F-2500, Hitachi).The wavelength of blue excitation light was 440 nm with slit width of 2.5 nm and emission was obtained through a slit width 2.5 nm with speed of 300 nm s^{-1}. Excitation spectrum was measured by monitoring at the 696 and 737 nm fluorescence peak of PSII and PSI, respectively.

3.5 Figures

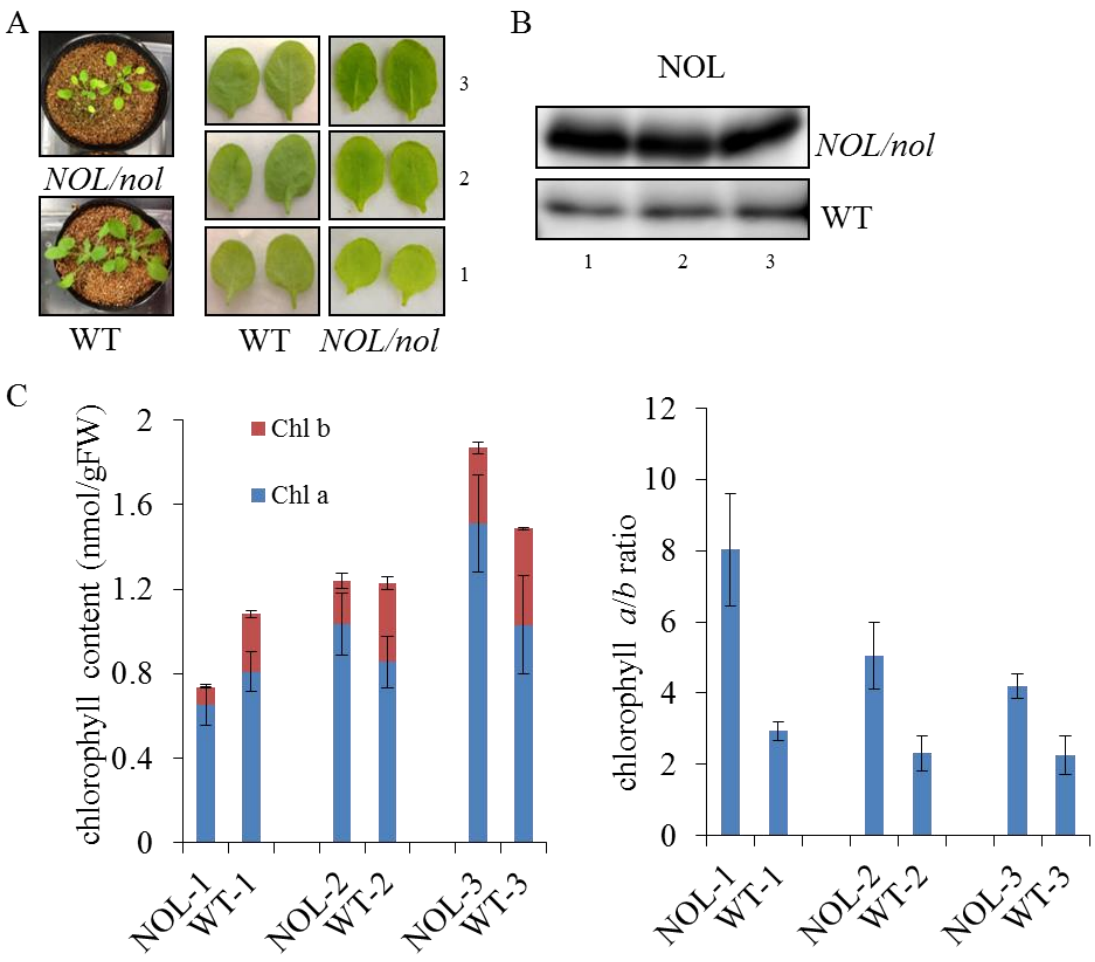

Figure 27. Chlorophyll and protein characteristic in different leaves. A, phenotype of NOL transformant plant. Detached leaves were respectively separated to oldest leaves, middle leaves and youngest leaves from bottom to upper of NOL/*nol* and WT in 3-4 weeks. B, imunant blotting analysis of NOL. Total proteins extracted from leaves were subjected to SDS-PAGE and NOL proteins were detected in WT and NOL/*nol* plants. C, analysis of chlorophyll content and chlorophyll *a*/*b* ratio. Chlorophyll was extracted from the matched leaves of NOL/*nol* and WT plants in different leaf stages and analyzed. Error bars represent ±SD (n=3). 1, 2, 3 mean old leaves, middle leaves and young leaves.

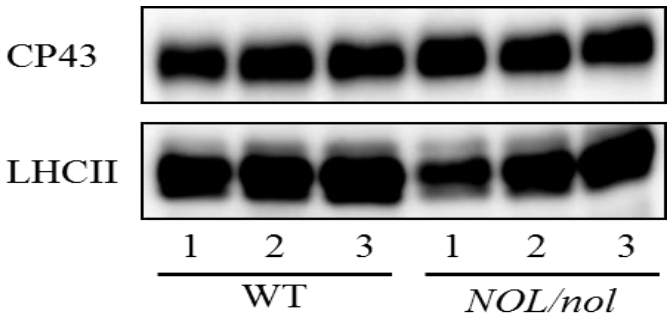

Figure 28. Changes of chlorophyll proteins. Total proteins extracted from leaves were subjected to SDS-PAGE and CP43 and LHCII proteins were detected.

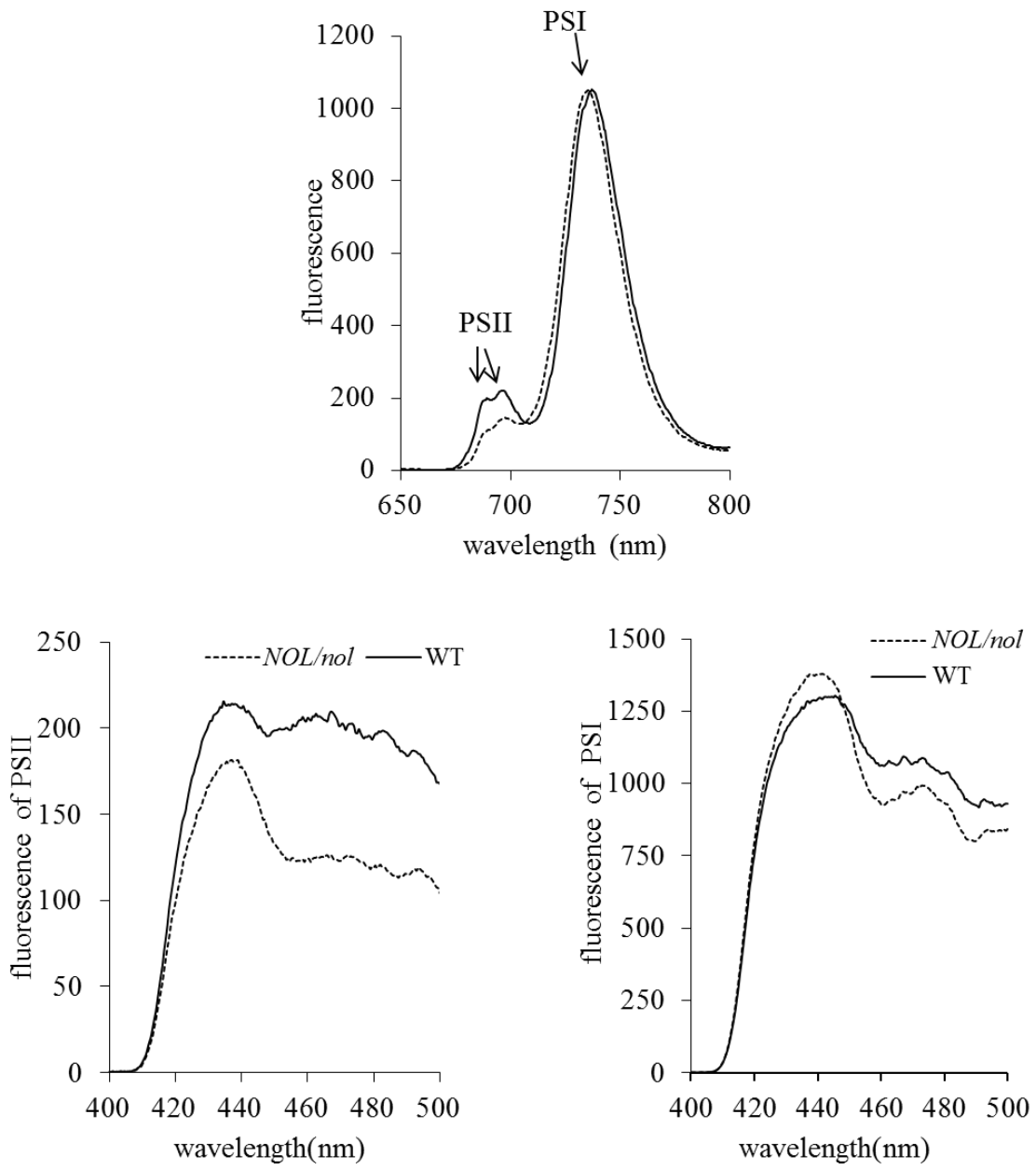

Figure 29. Spectra of the low temperature chlorophyll fluorescence. The fluorescence spectra of leaves from WT plant and NOL/*nol* plant at 77K were measured. The excitation wavelength was 440 nm.

Reference

1. Tanaka R, Tanaka A (2007) Tetrapyrrole biosynthesis in higher plants. *Annu Rev Plant Biol* 58:321–46.
2. Oster U, Tanaka R, Tanaka a, Rüdiger W (2000) Cloning and functional expression of the gene encoding the key enzyme for chlorophyll b biosynthesis (CAO) from Arabidopsis thaliana. *Plant J* 21(3):305–310.
3. Kusaba M, et al. (2007) Rice NON-YELLOW COLORING1 is involved in light-harvesting complex II and grana degradation during leaf senescence. *Plant Cell* 19(4):1362–1375.
4. Meguro M, Ito H, Takabayashi A, Tanaka R, Tanaka A (2011) Identification of the 7-hydroxymethyl chlorophyll a reductase of the chlorophyll cycle in Arabidopsis. *Plant Cell* 23:3442–3453.
5. Tanaka R, Tanaka A (2011) Chlorophyll cycle regulates the construction and destruction of the light-harvesting complexes. *Biochim Biophys Acta - Bioenerg* 1807(8):968–976.
6. Sakuraba Y, Balazadeh S, Tanaka R, Mueller-Roeber B, Tanaka A (2012) Overproduction of Chl b Retards Senescence Through Transcriptional Reprogramming in Arabidopsis. *Plant Cell Physiol* 53(3):505–517.
7. Horie Y, Ito H, Kusaba M, Tanaka R, Tanaka A (2009) Participation of chlorophyll b reductase in the initial step of the degradation of light-harvesting chlorophyll a/b-protein complexes in Arabidopsis. *J Biol Chem* 284(26):17449–56.
8. Wientjes E, Van Amerongen H, Croce R (2013) LHCII is an antenna of both photosystems after long-term acclimation. *Biochim Biophys Acta - Bioenerg*

1827(3):420–426.

9. Rochaix J-D, et al. (2012) Protein kinases and phosphatases involved in the acclimation of the photosynthetic apparatus to a changing light environment. *Philos Trans R Soc B Biol Sci* 367(1608):3466–3474.

10. Wilhelm C (1989) The energy distribution between the photosystems and light-induced changes in the stoichiometry of system I and II reaction centers in the chlorophyll b-containing alga Mantoniella squamata (Prasinophyceae). *Photosynth Res*:221–233.

11. Dietzel L, Bräutigam K, Pfannschmidt T (2008) Photosynthetic acclimation: State transitions and adjustment of photosystem stoichiometry - Functional relationships between short-term and long-term light quality acclimation in plants. *FEBS J* 275:1080–1088.

12. Anderson JM, Andersson B (1988) The dynamic photosynthetic membrane and regulation of solar energy conversion. *Trends Biochem Sci* 13(9):351–355.

13. Takahashi H, Iwai M, Takahashi Y, Minagawa J (2006) Identification of the mobile light-harvesting complex II polypeptides for state transitions in Chlamydomonas reinhardtii. *Proc Natl Acad Sci U S A* 103(2):477–482.

14. Depège N, Bellafiore S, Rochaix J-D (2003) Role of chloroplast protein kinase Stt7 in LHCII phosphorylation and state transition in Chlamydomonas. *Science* 299(5612):1572–1575.

15. Bellafiore S, Barneche F, Peltier G, Rochaix J-D (2005) State transitions and light adaptation require chloroplast thylakoid protein kinase STN7. *Nature* 433(7028):892–895.

16. Shapiguzov A, et al. (2010) The PPH1 phosphatase is specifically involved in LHCII dephosphorylation and state transitions in Arabidopsis. *Proc Natl Acad Sci* 107(10):4782–4787.

17. Pribil M, Pesaresi P, Hertle A, Barbato R, Leister D (2010) Role of Plastid Protein Phosphatase TAP38 in LHCII Dephosphorylation and Thylakoid Electron Flow. *PLoS Biol* 8(1):e1000288.

18. Niyogi KK (1998) Arabidopsis Mutants Define a Central Role for the Xanthophyll Cycle in the Regulation of Photosynthetic Energy Conversion. *Plant Cell Online* 10(7):1121–1134.

19. Külheim C, Agren J, Jansson S (2002) Rapid regulation of light harvesting and plant fitness in the field. *Science* 297(5578):91–3.

20. Horton P, Ruban A V, Walters RG (1996) Regulation of light harvesting in green plants. *Annu Rev Plant Physiol Plant Mol Biol* 47:655–684.

21. Bonente G, Howes BD, Caffarri S, Smulevich G, Bassi R (2008) Interactions between the Photosystem II Subunit PsbS and Xanthophylls Studied in Vivo and in Vitro. *J Biol Chem* 283(13):8434–8445.

22. Havaux M, Dall'Osto L, Bassi R (2007) Zeaxanthin Has Enhanced Antioxidant Capacity with Respect to All Other Xanthophylls in Arabidopsis Leaves and Functions Independent of Binding to PSII Antennae. *Plant Physiol* 145(4):1506–1520.

23. Tikkanen M, Grieco M, Aro E-M (2011) Novel insights into plant light-harvesting complex II phosphorylation and "state transitions." *Trends Plant Sci* 16(3):126–131.

24. Anderson JM, Chow WS, Park Y Il (1995) The grand design of

photosynthesis: Acclimation of the photosynthetic apparatus to environmental cues. *Photosynth Res* 46(1-2):129–139.

25. Melis A, et al. (1996) Chromatic regulation inChlamydomonas reinhardtii alters photosystem stoichiometry and improves the quantum efficiency of photosynthesis. *Photosynth Res* 47(3):253–265.

26. Fujita Y (1997) A study on the dynamic features of photosystem stoichiometry: Accomplishments and problems for future studies. *Photosynth Res* 53(2-3):83–93.

27. Kim JH, Glick RE, Melis a. (1993) Dynamics of Photosystem Stoichiometry Adjustment by Light Quality in Chloroplasts. *Plant Physiol* 102(1):181–190.

28. Pfannschmidt T, Allen JF, Oelmuller R (2001) Principles of redox control in photosynthesis gene expression. *Physiol Plant* 112(1):1–9.

29. Fey V, et al. (2005) Retrograde Plastid Redox Signals in the Expression of Nuclear Genes for Chloroplast Proteins of Arabidopsis thaliana. *J Biol Chem* 280(7):5318–5328.

30. Anderson JM (1986) PHOTOREGULATION OF THE COMPOSITION, FUNCTION, AND STRUCTURE OF THYLAKOID MEMBRANES. *An n Rev Plant Physiol* 37:93–136.

31. Chow WS, Melis a, Anderson JM (1990) Adjustments of photosystem stoichiometry in chloroplasts improve the quantum efficiency of photosynthesis. *Proc Natl Acad Sci U S A* 87(19):7502–7506.

32. Yamasato A, Nagata N, Tanaka R, Tanaka A (2005) The N-terminal domain of chlorophyllide a oxygenase confers protein instability in response to chlorophyll B accumulation in Arabidopsis. *Plant Cell* 17(5):1585–1597.

33. Hirashima M, Satoh S, Tanaka R, Tanaka A (2006) Pigment shuffling in antenna systems achieved by expressing prokaryotic chlorophyllide a oxygenase in Arabidopsis. *J Biol Chem* 281(22):15385–15393.

34. Bailey S, Walters RG, Jansson S, Horton P (2001) Acclimation of Arabidopsis thaliana to the light environment: the existence of separate low light and high light responses. *Planta* 213(5):794–801.

35. Hirashima M, Satoh S, Tanaka R, Tanaka A (2006) Pigment Shuffling in Antenna Systems Achieved by Expressing Prokaryotic Chlorophyllide a Oxygenase in Arabidopsis. *J Biol Chem* 281(22):15385–15393.

36. Tanaka R, Tanaka A (2005) Effects of chlorophyllide a oxygenase overexpression on light acclimation in Arabidopsis thaliana. *Photosynth Res* 85(3):327–340.

37. Thornber J, Highkin H (1974) Composition of the photosynthetic apparatus of normal barley leaves and a mutant lacking chlorophyll b. *Eur J Biochem* 41(1):109–116.

38. Bellemare G, Bartlett SG, Chua NH (1982) Biosynthesis of chlorophyll a/b-binding polypeptides in wild type and the chlorina f2 mutant of barley. *J Biol Chem* 257(13):7762–7767.

39. Król M, et al. (1995) Chlorophyll a/b-binding proteins, pigment conversions, and early light-induced proteins in a chlorophyll b-less barley mutant. *Plant Physiol* 107(3):873–83.

40. Bossmann B, Knoetzel J, Jansson S (1997) Screening of chlorina mutants of barley (Hordeum vulgare L.) with antibodies against light-harvesting proteins of PS I and PS II: Absence of specific antenna proteins. *Photosynth Res* 52(2):127–136.

41. Tzvetkova-Chevolleau T, et al. (2007) The light stress-induced protein ELIP2 is a regulator of chlorophyll synthesis in Arabidopsis thaliana. *Plant J* 50(5):795–809.

42. Takabayashi A, et al. (2011) The oligomeric states of the photosystems and the light-harvesting complexes in the Chl b-less mutant. *Plant Cell Physiol* 52(12):2103–14.

43. Schmid VHR (2002) Pigment Binding of Photosystem I Light-harvesting Proteins. *J Biol Chem* 277(40):37307–37314.

44. Schmid VHR (2008) Light-harvesting complexes of vascular plants. *Cell Mol Life Sci* 65(22):3619–39.

45. Caffarri S, Kouřil R, Kereïche S, Boekema EJ, Croce R (2009) Functional architecture of higher plant photosystem II supercomplexes. *EMBO J* 28(19):3052–3063.

46. Wientjes E, Croce R (2011) The light-harvesting complexes of higher-plant Photosystem I: Lhca1/4 and Lhca2/3 form two red-emitting heterodimers. *Biochem J* 433(3):477–85.

47. Ihalainen JA, et al. (2005) Excitation energy trapping in photosystem I complexes depleted in Lhca1 and Lhca4. *FEBS Lett* 579(21):4787–4791.

48. Xiaochun Qin, 1, 2* Michihiro Suga, 2* Tingyun Kuang, 1† Jian-Ren Shen1 2 (2015) Structural basis for energy transfer pathways in the plant PSI-LHCI supercomplex. 348(6238):989–995.

49. Homann H (1978) A Selective Effect of Mg * + on the Photochemistry at One Type of Reaction Center in Photosystem II of Chloroplasts ’. 190(2):523–530.

50. Terao T, Matsuoka M, Katoh S (1988) Immunological Quantification of Proteins Related to Light-Harvesting Chlorophyll a/b Protein Complexes of the Two Photosystems in Rice Mutants Totally and Partially Deficient in Chlorophyll b. *Plant Cell Physiol* 29 (5):825–834.

51. Bennett J (1977) Phosphorylation of chloroplast membrane polypeptides. *Nature* 269:344–346.

52. Ruban A V., Johnson MP, Duffy CDP (2012) The photoprotective molecular switch in the photosystem II antenna. *Biochim Biophys Acta - Bioenerg* 1817(1):167–181.

53. Krause GH, Weis E (1991) Chlorophyll Fluorescence and Photosynthesis: The Basics. *Annu Rev Plant Physiol Plant Mol Biol* 42(1):313–349.

54. Horton P, Ruban a. V. (1992) Regulation of Photosystem II. *Photosynth Res* 34:375–385.

55. Clough SJ, Bent AF (1998) Floral dip: A simplified method for Agrobacterium-mediated transformation of Arabidopsis thaliana. *Plant J* 16(6):735–743.

56. Hu X, Tanaka A, Tanaka R (2013) Simple extraction methods that prevent the artifactual conversion of chlorophyll to chlorophyllide during pigment isolation from leaf samples. *Plant Methods* 9(1):19.

57. Zapata M, Rodr ́guez F, Garrido JL (2000) Separation of chlorophylls and carotenoids from marine phytoplankton, a new HPLC method using a reversed phase C8 column and phridine-containing mobile phases. *Mar Ecol Prog Ser* 195:29–45.

58. Wittig I, Braun H-P, Sch ägger H (2006) Blue native PAGE. *Nat Protoc*

1(1):418–28.

59. Kim EH, et al. (2009) The multiple roles of light-harvesting chlorophyll a/b-protein complexes define structure and optimize function of Arabidopsis chloroplasts: a study using two chlorophyll b-less mutants. *Biochim Biophys Acta* 1787(8):973–984.

60. Shimada H, et al. (2005) Inactivation and deficiency of core proteins of photosystems I and II caused by genetical phylloquinone and plastoquinone deficiency but retained lamellar structure in a T-DNA mutant of Arabidopsis. *Plant J* 41(4):627–637.

61. Fuente JD La, Santiago J, Román A, Dumitrache C, Casasanto D (2014) When you think about it, your past is in front of you: How culture shapes spatial conceptions of time. *Psychol Sci* 25(9):1682–1690.

62. Hörtensteiner S (2006) Chlorophyll degradation during senescence. *Annu Rev Plant Biol* 57:55–77.

63. Meskauskiene R, et al. (2001) FLU: a negative regulator of chlorophyll biosynthesis in Arabidopsis thaliana. *Proc Natl Acad Sci U S A* 98(22):12826–12831.

64. Pružinská A, Tanner G, Anders I, Roca M, Hörtensteiner S (2003) Chlorophyll breakdown: pheophorbide a oxygenase is a Rieske-type iron-sulfur protein, encoded by the accelerated cell death 1 gene. *Proc Natl Acad Sci U S A* 100(25):15259–15264.

65. Tanaka R, Hirashima M, Satoh S, Tanaka A (2003) The Arabidopsis-accelerated cell death gene ACD1 is involved in oxygenation of pheophorbide a: inhibition of the pheophorbide a oxygenase activity does not lead to the “stay-green” phenotype in Arabidopsis. *Plant Cell Physiol*

44(12):1266–74.

66. Hirashima M, Tanaka R, Tanaka A (2009) Light-independent cell death induced by accumulation of pheophorbide a in Arabidopsis thaliana. *Plant Cell Physiol* 50(4):719–729.

67. Moon J, Zhu L, Shen H, Huq E (2008) PIF1 directly and indirectly regulates chlorophyll biosynthesis to optimize the greening process in Arabidopsis. *Proc Natl Acad Sci U S A* 105(27):9433–8.

68. Stenbaek A, Jensen PE (2010) Redox regulation of chlorophyll biosynthesis. *Phytochemistry* 71(8-9):853–859.

69. Liu X-G, et al. (2012) Effect of low temperature on chlorophyll biosynthesis in albinism line of wheat (Triticum aestivum) FA85. *Physiol Plant* 145(3):384–94.

70. Yang Q, et al. (2011) NOA1 functions in a temperature-dependent manner to regulate chlorophyll biosynthesis and Rubisco formation in rice. *PLoS One* 6(5):e20015.

71. Dalal VK, Tripathy BC (2012) Modulation of chlorophyll biosynthesis by water stress in rice seedlings during chloroplast biogenesis. *Plant Cell Environ* 35(9):1685–703.

72. Kobayashi K, et al. (2012) Regulation of Root Greening by Light and Auxin/Cytokinin Signaling in Arabidopsis. *Plant Cell* 24(3):1081–1095.

73. Hudson D, et al. (2011) GNC and CGA1 modulate chlorophyll biosynthesis and glutamate synthase (GLU1/Fd-GOGAT) expression in Arabidopsis. *PLoS One* 6(11):e26765.

74. Adhikari ND, et al. (2011) GUN4-Porphyrin Complexes Bind the

ChlH/GUN5 Subunit of Mg-Chelatase and Promote Chlorophyll Biosynthesis in Arabidopsis. *Plant Cell* 23(4):1449–1467.

75. Schottkowski M, Ratke J, Oster U, Nowaczyk M, Nickelsen J (2009) Pitt, a novel tetratricopeptide repeat protein involved in light-dependent chlorophyll biosynthesis and thylakoid membrane biogenesis in Synechocystis sp. PCC 6803. *Mol Plant* 2(6):1289–97.

76. Ito H, Ohtsuka T, Tanaka A (1996) Conversion of chlorophyll b to chlorophyll a via 7- hydroxymethyl chlorophyll. *JBiolChem* 271(3):1475–1479.

77. Rüdiger W (2002) Biosynthesis of chlorophyll b and the chlorophyll cycle. *Photosynth Res* 74(1998):187–193.

78. Espineda CE, Linford a S, Devine D, Brusslan J a (1999) The AtCAO gene, encoding chlorophyll a oxygenase, is required for chlorophyll b synthesis in Arabidopsis thaliana. *Proc Natl Acad Sci U S A* 96(18):10507–10511.

79. Tanaka a, et al. (1998) Chlorophyll a oxygenase (CAO) is involved in chlorophyll b formation from chlorophyll a. *Proc Natl Acad Sci U S A* 95(21):12719–23.

80. Sato Y, et al. (2009) Two short-chain dehydrogenase/reductases, NON-YELLOW COLORING 1 and NYC1-LIKE, are required for chlorophyll b and light-harvesting complex II degradation during senescence in rice. *Plant J* 57:120–131.

81. Ohtsuka T, Ito H, Tanaka a. (1997) Conversion of Chlorophyll b to Chlorophyll a and the Assembly of Chlorophyll with Apoproteins by Isolated Chloroplasts. *Plant Physiol* 113(1):137–147.

82. Tanaka A, Yamamoto Y, Tsuji H (1991) Formation of chlorophyll-protein complexes during greening. 2. Redistribution of chlorophyll among apoproteins. *Plant cell Physiol* 32(2):195–204.

83. Hörtensteiner S, Vicentini F, Matile P (1995) Chlorophyll breakdown in senescent cotyledons of rape, Brassica napus L.: enzymatic cleavage of phaeophorbide ain vitro. *New Phytol* 129(2):237–246.

84. Nakagawara E, Sakuraba Y, Yamasato A, Tanaka R, Tanaka A (2007) Clp protease controls chlorophyll b synthesis by regulating the level of chlorophyllide a oxygenase. *Plant J* 49(5):800–809.

85. Scheumann V, Schoch S, Rudiger W (1999) Chlorophyll b reduction during senescence of barley seedlings. *Planta* 209(3):364–70.

86. tomio Terao SK (1989) Synthesis and Breakdown of the Apoproteins of Light-Harvesting Chlorophyll a/b Proteins in Chlorophyll b-deficient Mutants of Rice. *Plant Cell Physiol* 30(4):571–580.

87. Flachmann R, Kühlbrandt W (1995) Post-Transcriptional Mechanisms in Tobacco. 7(February):149–160.

88. Zelisko A, García-Lorenzo M, Jackowski G, Jansson S, Funk C (2005) AtFtsH6 is involved in the degradation of the light-harvesting complex II during high-light acclimation and senescence. *Proc Natl Acad Sci U S A* 102(38):13699–13704.

89. Nakajima S, Ito H, Tanaka R, Tanaka A (2012) Chlorophyll b Reductase Plays an Essential Role in Maturation and Storability of Arabidopsis Seeds. *Plant Physiol* 160(1):261–273.

90. Shimoda Y, Ito H, Tanaka A (2012) Conversion of chlorophyll *b* to

chlorophyll *a* precedes magnesium dechelation for protection against necrosis in Arabidopsis. *Plant J* 72(3):501–511.

91. Sakuraba Y, Tanaka R, Yamasato A, Tanaka A (2009) Determination of a Chloroplast Degron in the Regulatory Domain of Chlorophyllide a Oxygenase. *J Biol Chem* 284(52):36689–36699.

92. Kunugi M, Takabayashi A, Tanaka A (2013) Evolutionary changes in chlorophyllide a oxygenase (CAO) structure contribute to the acquisition of a new light-harvesting complex in micromonas. *J Biol Chem* 288(27):19330–19341.

93. Ayumi Tanaka, yoshio Tanaka H tsuji (1987) Resolution of Chlorophyll a/b-Protein Complexes by Polyacrylamide Gel Electrophoresis: Evidence for the Heterogeneity of Light-Harvesting Chlorophyll a/b-Protein Complexes. *Plant Cell Physiol* 28(8):1537–1545.

94. Pribil M, Labs M, Leister D (2014) Structure and dynamics of thylakoids in land plants. *J Exp Bot* 65(8):1955–1972.

95. Dekker JP, Boekema EJ (2005) Supramolecular organization of thylakoid membrane proteins in green plants. *Biochim Biophys Acta - Bioenerg* 1706(1-2):12–39.

96. Belgio E, Johnson MP, Jurić S, Ruban AV (2012) Higher Plant Photosystem II Light-Harvesting Antenna, Not the Reaction Center, Determines the Excited-State Lifetime—Both the Maximum and the Nonphotochemically Quenched. *Biophys J* 102(12):2761–2771.

97. Gáspár L, Sárvári E, Morales F, Szigeti Z (2006) Presence of "PSI free" LHCI and monomeric LHCII and subsequent effects on fluorescence characteristics in lincomycin treated maize. *Planta* 223(5):1047–57.

98. Sakuraba Y, Yokono M, Akimoto S, Tanaka R, Tanaka A (2010) Deregulated Chlorophyll b Synthesis Reduces the Energy Transfer Rate Between Photosynthetic Pigments and Induces Photodamage in Arabidopsis thaliana. *Plant Cell Physiol* 51(6):1055–1065.

99. Lermontova I, Grimm B (2000) Overexpression of plastidic protoporphyrinogen IX oxidase leads to resistance to the diphenyl-ether herbicide acifluorfen. *Plant Physiol* 122(1):75–84.

100. Hellens RP, Anne Edwards E, Leyland NR, Bean S, Mullineaux PM (2000) pGreen: A versatile and flexible binary Ti vector for Agrobacterium-mediated plant transformation. *Plant Mol Biol* 42:819–832.

101. Earley KW, et al. (2006) Gateway-compatible vectors for plant functional genomics and proteomics. *Plant J* 45(4):616–629.

102. Croce R, van Amerongen H (2014) Natural strategies for photosynthetic light harvesting. *Nat Chem Biol* 10(7):492–501.

103. Nickelsen J, Rengstl B (2013) Photosystem II Assembly: From Cyanobacteria to Plants. *Annu Rev Plant Biol* 64(1):609–635.

104. Kouřil R, Dekker JP, Boekema EJ (2012) Supramolecular organization of photosystem II in green plants. *Biochim Biophys Acta* 1817(1):2–12.

105. Ayumi Tanaka YT and HT (1994) Preferential accumulation of apoproteins of the light-harvesting chlorophyll a/b-protein complex in greening barley leaves treated with 5-aminolevulinic acid on JSTOR. *Planta* 192(1):92–97.

106. Nick S, Meurer J, Soll J, Ankele E (2013) Nucleus-encoded light-harvesting chlorophyll a/b proteins are imported normally into chlorophyll b-free chloroplasts of arabidopsis. *Mol Plant* 6(3):860–871.

107. Park S-Y, et al. (2007) The senescence-induced staygreen protein regulates chlorophyll degradation. *Plant Cell* 19(5):1649–64.

108. Guiboileau A, Sormani R, Meyer C, Masclaux-Daubresse C (2010) Senescence and death of plant organs: Nutrient recycling and developmental regulation. *C R Biol* 333(4):382–391.

List of Publications

Ting Jia, H Ito, X Hu, A Tanaka. Accumulation of NON-YELLOW COLORING 1 protein of the chlorophyll cycle requires chlorophyll b in Arabidopsis thaliana. Plant Journal, 2015, 81(4), 586-596.

Ting Jia, H Ito, A Tanaka. The Chlorophyll b Reductase NOL Participates in Regulating the Antenna Size of Photosystem II in Arabidopsis Thaliana. Procedia Chemistry, 2015, 14:422-427

Acknowledgments

Research is a team work where firstly, I could not image having a better advisor and mentor for my ph.D. study, without their wide knowledge, perceptiveness I never can finish my study in 3 years. I am very fortunate to have their guidance. So here I wish to express my sincerely gratitude to my supervisors Prof. Ayumi Tanaka and Dr. Hisashi Ito for devoted guidance, pertinent advice, significant discussion, kindly suggestion and critical review throughout my PhD study and the writing of this thesis. And also thanks Prof. Junji Yamaguchi and Dr. Ryouichi Tanaka for support and encouragement during my research.

I am thankful to Dr. Hisashi Ito from bottom of my heart for his generous help at each step ranging from teaching techniques to discussion. I also deeply grateful to Dr. Atsushi Takabayashi for his patent support and advises. I also thank to Dr. Makio Yokono and Mrs. Yukako Kato to teach me perform the difficult experiments of photosystem antenna measurement and help me to solve problems during experiments and dada analysis. I am also very grateful to Mrs. Junko Kishimoto for her kind help as well as making my stay in japan every enjoying.In a short, I am greatly thankful to all members in Plant Adaption Biology Group and Hokkaido University for their assistance, help and friendliness.

This research was supported by Core Research for Evolutional Science and Technology, Japan Science and Technology Agency. The financial support by China Scholarship Council and Hokkaido University is gratefully acknowledged.

At the last but not the least I would like to express my heartfelt thanks to my parents and family for their encouragement, supporting and kindness in my life.

Ting Jia

Sapporo, January 2016